HHS Public Access

Author manuscript

ACS Infect Dis. Author manuscript; available in PMC 2022 May 14.

Published in final edited form as:

ACS Infect Dis. 2021 May 14; 7(5): 1089–1103. doi:10.1021/acsinfecdis.0c00508.

Novel congeners derived from microtubule-active phenylpyrimidines produce a potent and long-lasting paralysis of *Schistosoma mansoni in vitro*

Ludovica Monti[a], **Anne-Sophie Cornec**[b], **Killian Oukoloff**[a], **Jane Kovalevich**[c], **Kristen Prijs**[c], **Thibault Alle**[a], **Kurt R. Brunden**[c], **Amos B. Smith III**[b], **Nelly El-Sakkary**[a], **Lawrence J. Liu**[a], **Ali Syed**[a], **Danielle E. Skinner**[a], **Carlo Ballatore**[a,*], **Conor R. Caffrey**[a,*]

[a]Center for Discovery and Innovation in Parasitic Diseases (CDIPD), Skaggs School of Pharmacy and Pharmaceutical Sciences, University of California, San Diego, 9500 Gilman Drive, La Jolla, CA 92093

[b]Department of Chemistry, School of Arts and Sciences, University of Pennsylvania, 231 South 34th St., Philadelphia, PA 19104-6323

[c]Center for Neurodegenerative Disease Research, Perelman School of Medicine, University of Pennsylvania, 3600 Spruce Street, Philadelphia, PA 19104-6323

Abstract

Schistosomiasis is a parasitic disease that affects approximately 200 million people in developing countries. Current treatment relies on just one partially effective drug and new drugs are needed. Tubulin and microtubules (MTs) are essential constituents of the cytoskeleton in all eukaryotic cells and considered potential drug targets to treat parasitic infections. The α- and β-tubulin of *Schistosoma mansoni* have ~96% and ~91% sequence identity to their respective human tubulins suggesting that compounds which bind mammalian tubulin may interfere with MT-mediated functions in the parasite. To explore the potential of different classes of tubulin-binding molecules as anti-schistosomal leads, we completed a series of *in vitro* whole-organism screens of a target-based compound library against *S. mansoni* adults and somules (post-infective larvae), and identified multiple biologically active compounds, among which phenylpyrimidines were the most promising. Further structure-activity relationship studies of these hits identified a series of novel thiophen-2-yl-pyrimidine congeners, which induce a potent and long-lasting paralysis of the parasite. Moreover, compared to the originating compounds, which showed cytotoxicity values in the low nanomolar range, these new derivatives were 1 – 4 orders of magnitude less cytotoxic and exhibited weak or undetectable activity against mammalian MTs in a cell-based assay of MT stabilization. Given their selective anti-schistosomal activity and relatively simple drug-like

[*]**Corresponding Author Information** For C.B.: cballatore@health.ucsd.edu; For C.R.C.: ccaffrey@health.ucsd.edu.

Author Contributions

L.M., C.B., and C.R.C. conceived of the project. L.M., A.-S.C., K.O. and T.A. synthesized the compounds. A.B.S. III performed the data review and provided advice. LM., N.E.-S., L.J.L., A.S., D.E.S. and C.R.C. maintained the *S. mansoni* life cycle and performed the phenotypic assays. L.M. maintained HeLa and HEK293 cells *in vitro* and performed cytotoxicity assay. J.K., K.P. and K.R.B performed the tubulin assays. All authors contributed to the preparation and editing of the manuscript and have given approval to the final version of the manuscript.

The authors declare no competing financial interest.

structures, these molecules hold promise as candidates for the development of new treatments for schistosomiasis.

Graphical Abstract

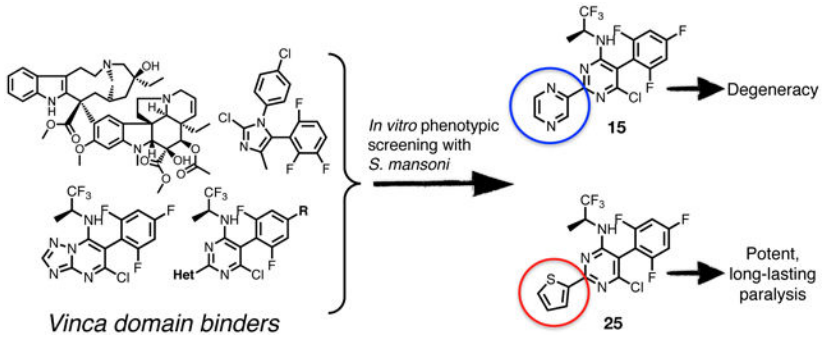

Keywords

Schistosoma mansoni ; schistosomiasis; drug discovery; tubulin; microtubule; phenylpyrimidines; structure-activity relationship

Introduction:

Schistosomiasis, also known as snail fever or bilharzia, is a chronic and morbid parasitic disease caused by trematode flatworms of the genus, *Schistosoma*. The major medically important species are *S. haematobium, S. mansoni* and *S. japonicum*.[1, 2] The disease is found in parts of the Middle East, South America, Southeast Asia and, particularly, sub-Saharan Africa. With approximately 200 million people infected and as many as 770 million at risk, [3,4] the disease is found among populations with inadequate sanitation and access to clean water.[5, 6] In spite of several efforts to develop vaccines for schistosomiasis, current therapy relies on a single drug, the pyrazinoisoquinoline derivative, praziquantel (PZQ).[4,7] Although PZQ is reasonably safe and effective,[7-9] the drug has notable sub-optimal features. For example, it is rarely curative at the single dose offered, suffers from a rapid metabolism into inactive metabolites,[7, 10, 11] and has limited efficacy against immature parasites, which prevents the use of the drug for chemoprophylaxis.[7, 12, 13] Moreover, the risk of possible emergence of resistance to PZQ remains a concern.[7, 9, 14, 15] The development of alternative treatments is clearly desirable. In this context, a potentially attractive, alternative drug target in schistosomes may be tubulin. Tubulin and microtubules (MTs) are essential constituents of the cytoskeleton in all eukaryotic cells and considered potential drug targets to treat parasitic diseases,[16] including schistosome infections.[17, 18] Tubulin is a highly conserved protein, and tubulin-containing structures (*i.e.*, MTs) are involved in many important cellular functions in all eukaryotic cells. In schistosomes, MTs play an essential role during membrane maturation, transport mechanisms, and secretory activities that support the survival of the parasites *in vitro* and *in vivo*.[17-19] Interestingly, α- and β-tubulin of *S. mansoni* exhibit significant amino acid sequence identity with eukaryotic tubulin orthologues, including those from humans (~96% and ~91% identity, respectively; Figure 1) suggesting that compounds which bind mammalian tubulin may

interfere with MT-mediated functions in the parasite. Based on their mode of action, MT-targeting compounds are typically divided in MT-stabilizing and -destabilizing agents, and form a remarkably broad and structurally diverse group of molecules that include different classes of natural products and non-naturally occurring small molecules.[20] A comprehensive evaluation of MT-active compounds from different classes as anti-schistosomal agents has not been conducted before.

To investigate the potential of tubulin/MT-binding agents as possible anti-schistosomal leads, we conducted an *in vitro* phenotypic screen of several representatives of a target-based library of MT-active compounds that interact with mammalian tubulin either at the colchicine,[21] vinblastine[22, 23] (vinca) or taxol[24] binding sites. This effort led to the identification of members of MT-active triazolopyrimidines and phenylpyrimidines that exhibit marked anti-schistosomal activity. Moreover, characterization of the structure-activity relationship (SAR) and further derivatization of the most promising phenylpyrimidine hits led to the discovery of novel thiophen-2-yl-pyrimidine congeners that produce a pronounced and long-lasting paralysis of the parasite *in vitro* at concentrations that are not toxic to rapidly dividing HeLa and HEK293 cells. Given their selective anti-schistosomal activity, combined with their relatively simple drug-like structures, these compounds offer novel starting points for the development of new treatments for schistosomiasis.

Results:

The compound collection tested in our initial screening (20 entries, Table 1) comprised molecules known to interact with mammalian tubulin either at the vinblastine (vinca), taxol and colchicine binding sites. In addition to representative examples of MT-stabilizing (*i.e.*, paclitaxel, **1**, and epothilone D, **2**), and -depolymerizing (*i.e.*, vinblastine, **3** and colchicine, **4**) natural products, several examples from non-naturally occurring classes of tubulin-interacting small molecules, such as the pyridopyrazine[29] (**5** and **6**), pyridazine[30] (**7** and **8**), imidazole[31] (**9** and **10**), triazolopyrimidine[32] (**11–14**) and phenylpyrimidine[33] (**15–20**) classes, were also included.

Test compounds were evaluated using whole-organism screens of two developmental stages of *S. mansoni* that infect humans, namely, adults (>42-days-old), which are responsible for disease pathology by the eggs they produce, and post-infective larvae (schistosomula or somules), which were freshly derived from infectious larvae (cercariae). The parasite's complex phenotypic responses to compound treatment, incorporating one or more changes relating to shape, density and motility were observed as a function of time and recorded using a constrained nomenclature of simple, and where possible, self-explanatory, descriptors, as previously described (Table 1 and see Experimental Section).[34-37] Descriptors and their associated severity scores were assessed at 1 and 10 μM compound concentrations for somules after 24 and 48 h, and at 5 μM for adults after 5, 24 and 48 h.

Compounds **1–4** exhibited relatively modest anti-schistosomal activity. Of these, the MT-stabilizing compounds **1** and **2** were comparatively more active (caused degeneracy) than the MT-depolymerizing agents, **3** and **4**, against somules at 10 μM. However, all four natural

products exhibited little or no activity when tested at 1 μM against somules and at 5 μM against adults (Table 1).

Among the non-naturally occurring small molecules, examples of the pyridazines (**7** and **8**) and imidazoles (**9** and **10**) demonstrated significant activity against both developmental stages. For example, these compounds produced degeneracy with severity scores as high as 4 when tested at 10 μM against somules. Also, compounds **7–10** induced uncoordinated movements and an inability of the adult parasite to adhere to the surface of the well floor that contributed to severity scores of 2 or 3. In contrast, the pyridopyrazines **5** and **6** were essentially devoid of anti-schistosomal activity (severity scores of ≤1; Table 1). The triazolopyrimidines (**11–14**) and phenylpyrimidines (**15–20**) generally produced high severity scores of up to 4 at both 10 and 1 μM against somules, whereas adults were more variably responsive with scores ranging from 0 to 4 (Figure 2A and B; Supplementary Video 2 for example responses of somules and adults, respectively, and Supplementary Video 1 for adult DMSO controls). Taken together, these screening data indicate that schistosomes are sensitive to MT-active compounds but that bioactivity depends on the class of molecules. This suggests that the anti-schistosomal SAR may be different or not fully overlapping with the anti-mitotic SAR in cancer cell lines.

Among the classes of MT-active compounds screened, the phenylpyrimidines were the most promising due to their relatively potent activity against both developmental stages of *S. mansoni*. Therefore, further SAR studies were focused on this class of compounds. Phenylpyrimidines are well studied as MT-stabilizing agents with promising anti-cancer activity both *in vitro* and *in vivo*.[3, 33] Several elements of the SAR that are necessary for their anti-mitotic activity are understood, including the critical importance of a nitrogen-containing heteroaromatic fragment linked at the C2 position of the pyrimidine scaffold.[33] Accordingly, to evaluate whether the observed anti-schistosomal activities of the phenylpyrimidines could be separated from MT-stabilizing and anti-mitotic activity in mammalian cells, a series of derivatives (**21–32**, Scheme 2 and Table 2) were synthesized and tested, including examples bearing structural modifications expected to attenuate MT-binding in mammalian cells.

Chemistry:

The synthesis of the phenylpyrimidine derivatives was performed following established procedures[33] as highlighted in Scheme 2. The pyrimidine ring was accessed via condensation reactions between the appropriately substituted diethylmalonate (**33** or **34**) and heteroaryl amidine (**35–39**). The resulting 4,6-dihydroxypyrimidines were then converted to the corresponding 4,6-dichlorides (**40–45**) upon treatment with phosphorus oxychloride. Finally, reaction with appropriate amines led to the final products **21–25** and **27–31** while the dehalogenated derivative, **26**, was obtained via hydrogenation from **25**. The deaminated derivative, **32**, was accessed by partial hydrogenolysis of the dichloride **44**. Compound **25** was a crystalline material that enabled X-ray diffraction analysis (Scheme 2).

Structure-activity relationships:

After synthesis, each of the test compounds was evaluated in the phenotypic assay for anti-schistosomal activity (Table 2). For these compounds, we also employed a camera-based assay called WormAssay[38, 39] that measures average adult worm motility per well. Finally, compounds were assessed in a previously described cell-based (HEK293) ELISA of MT-stabilization (Table 2).[40] Specifically, this assay measures compound-induced changes in the levels of acetylated α-tubulin (AcTub) in cell-lysates. Because AcTub is a known marker of stable MTs,[41, 42] the assay provides a convenient measure of MT-stabilizing activity of test compounds in the cellular *milieu*.[42]

As shown in Table 2, the phenylpyrimidine congeners equipped with *N*-containing heterocycles at C2, such as quinolin-2-yl (**21**), pyrazin-2-yl (**22**), and thiazol-2-yl (**23**), generally increased the AcTub levels in HEK293 cells by ~2–4-fold at 1 μM. This observation, which is in agreement with the anti-mitotic SAR,[33] confirms that **21–23** act as relatively potent MT-stabilizers of mammalian tubulin. Against the parasite, these phenylpyrimidines caused similar darker and uncoordinated changes in adult worms and/or degeneracy in somules as previously noted for the other potent MT-active congeners, **15–20**. In contrast, analogues bearing non-*N*-containing heteroaromatics at C2, such as furan-2-yl (**24**) and thiophen-2-yl (**25**), were less potent in the AcTub assay as indicated by the ~10-fold higher compound concentration, *i.e.*, 10 μM, required to obtain comparable elevations in AcTub levels (Table 2). Interestingly, although for **24**, the attenuation in MT-stabilizing activity in HEK293 cells appeared to correlate with a modest reduction in anti-schistosomal activity of the type already noted for **15–22**, in the case of thiophen-2-yl derivative, **25**, a strikingly different phenotype of paralysis (immobility) was recorded for both developmental stages at most of the time points and concentrations tested (Table 2; also, Figure 2C and Supplementary Video 3 for example responses of somules and adults, respectively).

Because of the striking combination of the worm paralysis phenotype and the attenuation of MT-stabilizing activity in mammalian cells, **25** was selected for further analogue design and testing. Thus, **26–32** (Scheme 2 and Table 2) included replacement (**28, 29** and **30**), removal (**32**) and inversion of the chiral configuration (**27**) of the amine fragment linked at C4, as well as dehalogenation at C6 (**26**) and removal of the fluorinated phenyl ring at C5 (**31**). Each of these modifications resulted in compounds that were unable to produce statistically significant elevations in AcTub levels in HEK293 cells at either 1 or 10 μM (Table 2). However, with the exception of the truncated analogues, **26, 31** and **32**, parasite paralysis of the type noted for **25** was observed for thiophen-2-yl congeners, **26–30**.

For adult parasites, the paralysis induced by **25, 28** and **29** was concentration-dependent with EC_{50} values of ~1 μM after 5 h as measured by WormAssay (Table 2 and Figure 3A). In addition, after extensive washing (6X exchange of the incubation volume), parasite motility was only partially recoverable depending on the compound and time of measurement after washing (Figure 3B and Supplementary Figure 1). Observationally, these worms had a severely decreased ability to flex and an inability to grasp the well floor with their suckers (Supplementary Video 4 for **28**) relative to age-matched

controls (Supplementary Video 5). These results suggest that the thiophen-2-yl analogues, exemplified by **25**, induce long-lasting and, possibly, irreversible damage to the parasite.

Finally, because of the weak or undetectable activity of the thiophene-2-yl derivatives in the HEK293 MT-stabilization assay, we reasoned that these phenylpyrimidines may be significantly less cytotoxic to rapidly dividing mammalian cells compared to closely related MT-active congeners. Indeed, the thiophene compounds **25–30** were 1–4 orders of magnitude less cytotoxic than the MT-active pyrazole (**22**) and thiazole (**23**) congeners in HEK293 and HeLa cell cytotoxicity assays (Table 3).

Discussion:

MT-targeting compounds have been widely investigated in cancer chemotherapy.[43] In addition, they are recognized as possible therapeutic agents to treat parasitic diseases, including schistosomiasis, as tubulin/MTs play essential roles during trematode growth and differentiation.[16, 44-46] The high level of identity observed between human and schistosomal tubulin sequences provides the basis for assessing the anti-schistosomal activity of different classes of compounds that are known to interact with mammalian tubulin/MTs.

To investigate the potential of tubulin-interacting compounds as anti-schistosomal leads, we evaluated in phenotypic screens of *S. mansoni* a collection of MT-active molecules from different compound classes. For two developmental stages of the parasite, the phenotypic screens identified several synthetic MT-active heterocycles that induced a variety of phenotypic responses (Table 1). In particular, the triazolopyrimidines (*e.g.*, **12**) and phenylpyrimidines (*e.g.*, **19** and **20**), which interact with mammalian tubulin at the vinca domain (*i.e.*, vinblastine binding site)[23] and possess potent anti-mitotic effects against mammalian cells,[32, 33] were among the most effective anti-schistosomals.

Although the data demonstrate that *S. mansoni* is sensitive to MT-targeting agents, any clinical application of these potent anti-mitotic compounds for the treatment of infection would be faced with the possibility of host toxicity that might ultimately result in dose-limiting side-effects. This aspect is of particular importance in the case of schistosomiasis for which the current drug, PZQ, is employed in communities with minimal medical supervision. Interestingly, although the amino acid residues comprising the vinblastine site are all conserved in schistosome tubulin (Figure 1), our screening data showed that different vinca domain binders (*i.e.*, **3, 5–20**) can in fact be variously active and/or produce drastically different phenotypic responses. Moreover, our results revealed that the anti-mitotic activity of these compounds in mammalian cells does not always correlate with anti-schistosomal activity suggesting that differences may exist between mammalian cells and the parasite that could be exploited to identify selective anti-schistosomal agents.

To investigate whether the anti-schistosomal activity of these compounds could be separated from the anti-mitotic effects against mammalian cells, a focused set of phenylpyrimidine analogues was synthesized. The set included examples that featured specific structural changes that were expected to attenuate MT-stabilizing activity in mammalian cells. This effort identified phenylpyrimidines bearing a thiophen-2-yl fragment at C2, *i.e.*, **25–32**,

that (i) showed either a weak or undetectable ability to alter markers of stable MTs in HEK293 cells, (ii) were 1 – 4 orders of magnitude less toxic to HeLa and HEK293 cells, and (iii) yet rapidly and potently paralyzed both developmental stages of *S. mansoni* with EC_{50} values in the low μM range. Moreover, the paralysis induced was only partially reversible suggesting a long-lasting and, perhaps, permanent duration of action, which, under the dynamic of the host-parasite relationship *in vivo*, might impair the parasite's ability to maintain position in the blood system and prove ultimately detrimental to parasite survival. These results demonstrate that even minor modifications, as small as a single atom replacement, in the structure of phenylpyrimidine MT-targeting agents (*cf.*, **23** and **25**) result in derivatives that exhibit selective anti-schistosomal activity. Although the phenotypic screen data do not provide a detailed insight into the mechanism of action of thiophen-2-yl-pyrimidines and their interaction with parasite tubulin/MTs has not yet been investigated, our findings suggest that, compared to their originating MT-binder congeners, the thiophen-2-yl-pyrimidine derivatives may either interact selectively with parasite tubulin and/or potentially engage one or more targets other than tubulin/MTs.

Conclusions:

Phenotypic screening of a series of compounds known to target mammalian tubulin/MTs with the schistosome parasite identified different members of MT-active triazolopyrimidines and phenylpyrimidines with marked anti-schistosomal activity. An assessment of the anti-schistosomal SAR of phenylpyrimidines was conducted and compared with the previously established MT-stabilizing and anti-mitotic SAR. This effort led to the synthesis, testing and identification of structurally related thiophen-2-yl congeners that produce a rapid, potent and sustained paralysis of the parasite at concentrations that do not cause significant MT-stabilization or cytotoxicity in mammalian cells. Compounds of this type could form the basis for the development of novel anti-schistosomal therapeutics.

Experimental section:

Sequence retrieval, alignment and phylogenetic analysis.

Sequence data were obtained from the NCBI refseq database (accession numbers provided in parentheses). *Homo sapiens alpha* (AAA91576.1) and *beta* (AAC52035.1) tubulin sequences were used to query the NCBI refseq database using BLASTP.[47] MUSCLE[25, 26] was used to build a multiple sequence alignment of α- and β-tubulin amino acid sequences from *Schistosoma mansoni* (XP_018652548.1, XP_018652475.1), *S. haematobium* (KAF1333866.1, XP_012794904.1), *S. japonicum* (CAX72946.1, TNN06284.1), *Drosophila pseudoobscura* (XP_001359737.1, XP_001357842.1), *Caenorhabditis elegans* (BAA22203.1, NP_509585.1), and *Homo sapiens* (AAA91576.1, AAC52035.1). A maximum likelihood tree was inferred from a multiple sequence alignment of full-length tubulin sequences using IQ-TREE2[27] (v 2.0.6) and was midpoint-rooted. The phylogenetic tree and alignment were then visualised using the interactive tree of life program (iTOL; https://itol.embl.de).[28]

Chemistry.

All solvents were reagent grade. All reagents were purchased from Aldrich or Acros and used as received. Thin layer chromatography (TLC) was performed with 0.25 mm E. Merck precoated silica gel plates. Silica gel column chromatography was performed with silica gel 60 (particle size 0.040–0.062 mm) supplied by Silicycle and Sorbent Technologies. TLC spots were detected by viewing under a UV light. Melting points (mp) were acquired on a Mel-Temp II (model: 1001) and are uncorrected. Infrared (IR) spectra were recorded on a Bruker, model Alpha spectrometer (part number 1003271/03). Proton (^{1}H) and Carbon (^{13}C) NMR spectra were recorded on a 500 MHz Bruker AMX-500 spectrometer or 600 MHz Bruker Avance III spectrometer. Chemical shifts were reported relative to solvents. High-resolution mass spectra were measured using an Agilent 6230 time-of-flight mass spectrometer (TOFMS) with Jet stream electrospray ionisation source (ESI). Single-crystal X-ray structure determinations were performed Bruker MicroStar with an APEX II detector, double-bounce micro-focus optics and a Cu rotating anode source. Analytical reverse-phase (Sunfire C18; 4.6 mm × 50 mm, 5 mL) high-performance liquid chromatography (HPLC) was performed with a Gilson HPLC equipped with UV and mass detector. All samples were analysed employing a linear gradient from 10% to 90% of CH_3CN in water over 8 min and flow rate of 1 mL/min, and unless otherwise stated, the purity level was >95%. Preparative reverse-phase HPLC purifications were performed on a Gilson instrument employing Waters SunFire preparative C_{18} OBD columns (5 μm 19 mm μ 50 mm or 19 mm – 100 mm). Purifications were carried out employing a linear gradient from 10% to 90% of CH_3CN in water with 0.1% formic acid for 15 min with a flow rate of 20 mL/min. Compounds **1, 3, 4** were commercially available, whereas **3, 5–20**, had been synthesized previously in our laboratories as part of a drug discovery program for Alzheimer's disease.[40, 48, 49] Unless otherwise stated, all final compounds were found to be >95% pure as determined by HPLC/MS and NMR.

(S)-6-chloro-2-(quinolin-2-yl)-5-(2,4,6-trifluorophenyl)-N-(1,1,1-trifluoropropan-2-yl)pyrimidin-4-amine (21).—To a solution of 2-(4,6-dichloro-5-(2,4,6-trifluorophenyl)pyrimidin-2-yl)quinoline (**40**) (0.122 g, 0.30 mmol, 1 equiv) in DMF (2.6 mL) were added (*S*)-1,1,1-trifluoropropan-2-amine hydrochloride (0.179 g, 1.20 mmol, 4 equiv) and *N,N*-diisopropylethylamine (0.155 g, 1.20 mmol, 4 equiv). The reaction mixture was stirred at 90 °C for 40 h, then partitioned between EtOAc and brine. The aqueous phase was extracted with EtOAc (×3), and the combined organic layers were washed with brine (×2), dried over $MgSO_4$, filtered and concentrated. Purification by reverse-phase HPLC afforded the title compound as a white solid (0.022 g, 0.046 mmol, 15%). ^{1}H NMR (500 MHz; $CDCl_3$) δ 8.48 (d, J = 8.5 Hz, 1H), 8.37 (d, J = 8.5 Hz, 1H), 8.32 (d, J = 8.6 Hz, 1H), 7.89 (d, J = 8.1 Hz, 1H), 7.77 (td, J = 7.7, 1.3 Hz, 1H), 7.63–7.60 (m, 1H), 6.88 (dtt, J = 7.6, 5.1, 2.6 Hz, 2H), 5.45–5.38 (m, 1H), 4.65 (d, J = 9.2 Hz, 1H), 1.44 (d, J = 7.0 Hz, 3H) ppm; ^{13}C NMR (126 MHz; $CDCl_3$) δ 164.25 (dt, J = 253.8, 15.0 Hz), 163.78, 161.62, 161.21, 160.94 (dddd, J = 252.7, 14.5, 9.1, 2.0 Hz), 153.79, 148.25, 137.07 , 131.08, 129.92, 128.88, 127.93, 127.56, 126.64, 124.40, 120.99, 105.20 (td, J = 21.0, 4.8 Hz), 104.24, 101.74 (tdd, J = 25.3, 20.3, 4.6 Hz), 48.31 (q, J = 31.5 Hz), 14.63 ppm; IR (KBr)

ν 3432, 3265, 3121, 3004, 2953, 2924, 1637, 1575, 1557, 1402, 1275, 1180, 1141, 1122 cm^{-1}; HRMS (ES^+) calculated for $C_{22}H_{14}ClF_6N_4$ $[M + H]^+$ 483.0811, found 483.0814.

6-chloro-N-((3-methyl-3H-diazirin-3-yl)methyl)-2-(pyrazin-2-yl)-5-(2,4,6-trifluorophenyl)-pyrimidin-4-amine (22).—To a solution of 4,6-dichloro-2-(pyrazin-2-yl)-5-(2,4,6-trifluorophenyl)pyrimidine (**41**) (0.030 g, 0.084 mmol, 1 equiv) in anhydrous DMF (1.8 mL) (3-methyl-3H-diazirin-3-yl)methanamine hydrochloride[50] (0.011 g, 0.092 mmol, 1.1 equiv) and *N,N*-diisopropylethylamine (0.032 g, 0.252 mmol, 3 equiv) were added and the reaction mixture was stirred at RT for 3h. Then water was added and extracted with EtOAc (×2). The combined organic layers were washed with brine (x3), dried over $MgSO_4$, filtered and concentrated in vacuo. Purification by flash chromatography (hexanes/EtOAc 100:0 to 60:40) afforded the title compound as a light brown solid (0.026 g, 0.064 mmol, 76%). ^1H NMR (600 MHz, $CDCl_3$) δ 9.76 (d, J = 0.6 Hz, 1H), 8.77 (d, J = 1.5 Hz, 1H), 8.70 (d, J = 2.4 Hz, 1H), 6.75 (t, J = 7.8 Hz, 2H), 5.31 (t, J = 5.9 Hz, 1H), 3.61 (d, J = 6.2 Hz, 2H), 1.12 (s, 3H) ppm; ^{13}C NMR (151 MHz, $CDCl_3$) δ 164.00 (dt, J = 253.5, 15.1 Hz), 161.63, 161.58, 160.87 (ddd, J = 252.9, 15.0, 9.1 Hz), 160.77, 149.25, 145.99, 145.68, 144.44, 105.33 (td, J = 20.9, 4.6 Hz), 101.90–100.98 (m), 44.83, 25.68, 18.13 ppm; IR ν 3275, 1547, 1512, 1395, 1190, 1107, 820, 694 cm^{-1}; HRMS (ES^+) calculated for $C_{17}H_{11}ClF_3N_7$ $[M + H]^+$ 406.0789, found 406.0791.

(S)-6-chloro-2-(thiazol-2-yl)-5-(2,4,6-trifluorophenyl)-N-(1,1,1-trifluoropropan-2-yl)pyrimidin-4-amine (23).—Synthesized as **21**, starting from 2-(4,6-dichloro-5-(2,4,6-trifluorophenyl)pyrimidin-2-yl)thiazole (**42**) (0.179 g, 0.494 mmol), (*S*)-1,1,1-trifluoropropan-2-amine hydrochloride (0.296 g, 1.98 mmol) and *N,N*-diisopropylethylamine (0.256 g, 1.98 mmol). Reaction mixture was stirred at 90 °C for 18 h. Purification by silica gel column chromatography (hexanes/EtOAc 80:20) afforded the title compound as a white solid (0.065 g, 0.148 mmol, 30%). ^1H NMR (600MHz, $CDCl_3$) δ 8.00 (d, J = 3.2 Hz, 1H), 7.54 (d, J = 3.2 Hz, 1H), 6.78–6.70 (m, 2H), 5.35–5.28 (m, 1H), 5.28–5.23 (m, 1H), 1.39 (d, J = 6.8 Hz, 3H) ppm; ^{13}C NMR (151 MHz, $CDCl_3$) δ 165.71, 164.06 (dt, J = 254.1, 15.5 Hz), 161.13, 160.90, 161.98–159.67 (m), 158.55, 145.22, 125.45 (q, J = 283.2, 280.1 Hz), 123.74, 105.02 (td, J = 20.5, 5.2 Hz), 104.35, 102.47–99.18 (m), 48.24 (q, J = 31.4 Hz), 14.22 ppm; IR (KBr) ν 1578, 1554, 1544, 1439, 1272, 1148, 1121, 1032, 796 cm^{-1}; HRMS (ES^+) calculated for $C_{16}H_{10}ClF_6N_4S$ $[M + H]^+$ 439.0213, found 439.0207.

(S)-6-chloro-2-(furan-2-yl)-5-(2,4,6-trifluorophenyl)-N-(1,1,1-trifluoropropan-2-yl)pyrimidin-4-amine (24).—Synthesized as **21**, starting from 4,6-dichloro-2-(furan-2-yl)-5-(2,4,6-trifluorophenyl)pyrimidine (**43**) (0.076 g, 0.22 mmol), (*S*)-1,1,1-trifluoropropan-2-amine hydrochloride (0.132 g, 0.88 mmol) and *N,N*-diisopropylethylamine (0.114 g, 0.88 mmol). Reaction mixture was stirred at 90 °C for 40 h. Purification by reverse-phase HPLC afforded the title compound as a beige solid (0.021 g, 0.050 mmol, 23%). ^1H NMR (500 MHz; $CDCl_3$) δ 7.63–7.63 (m, 1H), 7.35 (dd, J = 3.4, 0.7 Hz, 1H), 6.89–6.83 (m, 2H), 6.56 (dd, J = 3.5, 1.7 Hz, 1H), 5.32–5.22 (m, 1H), 4.50 (d, J = 9.4 Hz, 1H), 1.38 (d, J = 7.0 Hz, 3H) ppm; ^{13}C NMR (126 MHz; $CDCl_3$) δ 164.15 (dt, J = 253.5, 15.0 Hz), 161.06 (ddd, J = 252.1,

9.3, 4.1 Hz), 160.95 (ddd, J = 252.6, 9.1, 3.7 Hz), 160.76, 160.49, 157.04, 151.15, 145.80, 125.47 (q, J = 281.6 Hz), 115.18, 112.39, 105.30 (td, J = 21.0, 4.8 Hz), 102.14, 101.64 (tdd, J = 25.7, 21.3, 4.3 Hz), 90.49, 56.76, 50.42, 48.05 (q, J = 31.6 Hz), 14.61 (d, J = 1.5 Hz) ppm; IR (KBr) ν 3320, 2999, 2962, 2919, 2857, 1636, 1594, 1550, 1490, 1183, 1144, 1123 cm^{-1}; HRMS (ES^+) calculated for $C_{17}H_{11}ClF_6N_3O$ $[M + H]^+$ 422.0495, found 422.0499.

(S)-6-chloro-2-(thiophen-2-yl)-5-(2,4,6-trifluorophenyl)-N-(1,1,1-trifluoropropan-2-yl)pyrimidin-4-amine (25).—Synthesized as **21**, starting from 4,6-dichloro-2-(thiophen-2-yl)-5-(2,4,6-trifluorophenyl)pyrimidine (**44**) (0.067 g, 0.18 mmol), (*S*)-1,1,1-trifluoropropan-2-amine hydrochloride (0.110 g, 0.74 mmol) and *N,N*-diisopropylethylamine (0.096 g, 0.74 mmol). Reaction mixture was stirred at 90 °C for 72 h. Purification by reverse-phase HPLC afforded the title compound as a white solid (0.024 g, 0.055 mmol, 30%). X-ray quality crystals were obtained by slow evaporation from a diethyl ether/pentane solution (see Supporting Information): mp (diethyl ether/pentane) 121–123 °C. CCDC 1946855. ^{1}H NMR (600 MHz, $CDCl_3$) δ 8.02 (d, J = 3.7 Hz, 1H), 7.51 (d, J = 5.0 Hz, 1H), 7.14 (t, J = 4.4 Hz, 1H), 6.92–6.84 (m, 2H), 5.31–5.19 (m, 1H), 4.44 (d, J = 9.4 Hz, 1H), 1.39 (d, J = 7.0 Hz, 3H) ppm; ^{13}C NMR (151 MHz, $CDCl_3$) δ 164.07 (dt, J = 253.4, 15.2 Hz), 160.99 (ddd, J = 252.8, 9.7, 5.5 Hz), 160.88 (ddd, J = 246.8, 8.3, 5.9 Hz), 160.87, 160.46, 160.30, 142.02, 131.04, 130.39, 128.37, 125.44 (q, J = 281.6 Hz), 105.28 (td, J = 21.1, 4.2 Hz), 101.66 (qd, J = 25.8, 4.2 Hz), 48.02 (q, J = 31.7 Hz), 14.61 ppm; IR (KBr) ν 3353, 2923, 1637, 1556, 1527 cm^{-1}; HRMS (ES^+) calculated for $C_{17}H_{11}ClF_6N_3S$ $[M + H]^+$ 438.0261, found 438.0262.

(S)-2-(thiophen-2-yl)-5-(2,4,6-trifluorophenyl)-N-(1,1,1-trifluoropropan-2-yl)pyrimidin-4-amine (26).—To a solution of (*S*)-6-chloro-2-(thiophen-2-yl)-5-(2,4,6-trifluorophenyl)-*N*-(1,1,1-trifluoropropan-2-yl)pyrimidin-4-amine (**25**) (0.020 g, 0.046 mmol, 1 equiv) in degassed MeOH (1 mL) was added sodium acetate (0.0075 g, 0.091 mmol, 2 equiv) and Palladium on carbon 10 wt.% (0.030 g, 0.028 mmol, 0.6 equiv). Hydrogen was bubbled in the solution and reaction mixture was stirred under hydrogen atmosphere at room temperature for 48 hours. Then, mixture was filtered, concentrated and the crude was purified by silica gel column chromatography (hexanes/EtOAc 97:3) to obtain the title compound as a white solid (0.004 g, 0.001 mmol, 22%). ^{1}H NMR (600 MHz, $CDCl_3$) δ 8.16 (s, 1H), 7.99 (d, J = 3.6 Hz, 1H), 7.48 (d, J = 5.0 Hz, 1H), 7.14 (t, J = 4.4 Hz, 1H), 6.90–6.84 (m, 2H), 5.39–5.28 (m, 1H), 4.46 (d, J = 9.3 Hz, 1H), 1.41 (d, J = 7.0 Hz, 3H). ^{13}C NMR (151 MHz, $CDCl_3$) δ 160.98, 158.67, 157.55, 143.38, 130.07, 129.23, 128.37 (d, J = 26.0 Hz), 128.76–121.25 (m), 104.04, 101.61 (qd, J = 26.1, 4.2 Hz), 47.30 (q, J = 31.3 Hz), 14.68 ppm; IR (KBr) ν 1572, 1562, 1439, 1376, 1137, 1120, 1032 cm^{-1}; HRMS (ES^+) calculated for $C_{17}H_{12}F_6N_3S$ $[M + H]^+$ 404.0651, found 404.0648.

(R)-6-chloro-2-(thiophen-2-yl)-5-(2,4,6-trifluorophenyl)-N-(1,1,1-trifluoropropan-2-yl)pyrimidin-4-amine (27).—Synthesized as **21**, starting from 4,6-dichloro-2-(thiophen-2-yl)-5-(2,4,6-trifluorophenyl)pyrimidine (**44**) (0.077 g, 0.213 mmol), (*R*)-1,1,1-trifluoropropan-2-amine (0.127 g, 0.853 mmol) and *N,N*-diisopropylethylamine (0.110 g, 0.853 mmol). Purification by silica gel column chromatography (hexanes/EtOAc 100:0 to 90:10)

afforded the title compound as a white solid (0.013 g, 0.030 mmol, 14%). ^{1}H NMR (600 MHz, $CDCl_3$) δ 8.02 (dd, J = 3.7, 1.3 Hz, 1H), 7.51 (dd, J = 5.0, 1.2 Hz, 1H), 7.14 (dd, J = 5.0, 3.7 Hz, 1H), 6.92–6.84 (m, 2H), 5.31–5.19 (m, 1H), 4.44 (d, J = 9.3 Hz, 1H), 1.39 (d, J = 7.0 Hz, 3H) ppm; ^{13}C NMR (151 MHz, $CDCl_3$) δ 164.07 (dt, J = 253.2, 15.1 Hz), 161.97–161.58 (m), 160.88, 160.46, 160.31, 160.11 (ddd, J = 14.9, 8.8, 5.7 Hz), 142.03, 131.03, 130.39, 128.36, 125.43 (q, J = 281.6 Hz), 105.51–104.95 (m), 102.00–101.25 (m), 48.03 (q, J = 31.5 Hz), 14.61 ppm; IR (KBr) ν 1674, 1593, 1579, 1554, 1440, 1395, 1140, 1121, 1035 cm^{-1}; HRMS (ES^+) calculated for $C_{17}H_{11}ClF_6N_3S$ $[M + H]^+$ 438.0261, found 438.0261.

(R)-6-chloro-N-(3-methylbutan-2-yl)-2-(thiophen-2-yl)-5-(2,4,6-trifluorophenyl)pyrimidin-4-amine (28).—To a solution of 4,6-dichloro-2-(thiophen-2-yl)-5-(2,4,6-trifluorophenyl)pyrimidine (**44**) (0.100 g, 0.277 mmol) in anhydrous DMF (2.0 mL) was added (*R*)-3-methylbutan-2-amine (0.051 g, 0.581 mmol) and the reaction mixture was stirred at room temperature for 1 h. Then water was added and the mixture was extracted with EtOAc (×2). The organic layers were washed with brine (×3), dried over $MgSO_4$, filtered and concentrated. Purification by silica gel column chromatography (hexanes/EtOAc 98:2) afforded the title compound as a white solid (0.123 g, 0.026 mmol, 89%). ^{1}H NMR (600 MHz, $CDCl_3$) δ 7.99 (dd, J = 3.8, 1.5 Hz, 1H), 7.47 (dd, J = 5.1, 1.5 Hz, 1H), 7.12 (dd, J = 5.0, 3.6 Hz, 1H), 6.86 (t, J = 8.1 Hz, 2H), 4.31 (d, J = 8.6 Hz, 1H), 4.30–4.22 (m, 1H), 1.87–1.78 (m, 1H), 1.12 (d, J = 6.5 Hz, 3H), 0.88 (dd, J = 6.9, 3.7 Hz, 6H) ppm; ^{13}C NMR (151 MHz, $CDCl_3$) δ 163.69 (dt, J = 252.4, 15.0 Hz), 160.95 (dddd, J = 251.5, 29.8, 15.0, 9.2 Hz), 160.87, 160.84, 159.12, 142.84, 130.30, 129.65, 128.12, 106.09 (td, J = 21.2, 4.9 Hz), 101.37 (tdd, J = 25.9, 21.5, 4.0 Hz), 100.74, 52.01, 32.83, 18.51, 18.27, 17.16 ppm; IR (KBr) ν 1568, 1554, 1432, 1395, 1121, 1001, 842 cm^{-1}; HRMS (ES^+) calculated for $C_{19}H_{18}ClF_3N_3S$ $[M + H]^+$ 412.0857, found 412.0852.

(S)-6-chloro-N-(3-methylbutan-2-yl)-2-(thiophen-2-yl)-5-(2,4,6-trifluorophenyl)pyrimidin-4-amine (29).—Synthesized as **28**, starting from 4,6-dichloro-2-(thiophen-2-yl)-5-(2,4,6-trifluorophenyl)pyrimidine (**44**) (0.100 g, 0.277 mmol) and (*S*)-3-methylbutan-2-amine (0.051 g, 0.581 mmol). Purification by silica gel column chromatography (hexanes/EtOAc 98:2) afforded the title compound as a white solid (0.092 g, 0.022 mmol, 71%). ^{1}H NMR (600 MHz, $CDCl_3$) δ 8.00 (d, J = 3.7 Hz, 1H), 7.47 (d, J = 5.0 Hz, 1H), 7.12 (t, J = 4.3 Hz, 1H), 6.85 (t, J = 8.2 Hz, 2H), 4.33 (d, J = 8.4 Hz, 1H), 4.31–4.24 (m, 1H), 1.87–1.79 (m, J = 6.8 Hz, 1H), 1.13 (d, J = 6.8 Hz, 3H), 0.91–0.86 (m, 6H) ppm; ^{13}C NMR (151 MHz, $CDCl_3$) δ 163.73 (dt, J = 252.5, 15.0 Hz), 161.00 (dddd, J = 251.7, 29.0, 14.9, 9.0 Hz), 160.91, 160.89, 159.17, 142.88, 130.35, 129.70, 128.17, 106.13 (td, J = 21.0, 4.6 Hz), 101.43 (tdd, J = 26.0, 22.0, 4.2 Hz), 100.78, 52.02, 32.87, 18.55, 18.31, 17.22 ppm; IR (KBr) ν 1569, 1553, 1432, 1394, 1120, 1031, 842 cm^{-1}; HRMS (ES^+) calculated for $C_{19}H_{18}ClF_3N_3S$ $[M + H]^+$ 412.0857, found 412.0857.

6-chloro-N-((3-methyl-3H-diazirin-3-yl)methyl)-2-(thiophen-2-yl)-5-(2,4,6-trifluorophenyl)-pyrimidin-4-amine (30).—Synthesized as **22**, starting from 4,6-dichloro-2-(thiophen-2-yl)-5-(2,4,6-trifluorophenyl)pyrimidine (**44**) (0.059 g, 0.16 mmol), (3-methyl-3H-diazirin-3-yl)methanamine hydrochloride[50] (0.040 g, 0.33 mmol) and triethylamine (0.067 g, 0.66 mmol,

4 equiv). Purification by reverse-phase HPLC afforded the title compound as a white solid (0.019 g, 0.046 mmol, 28%). ^{1}H NMR (600 MHz, $CDCl_3$) δ 8.08 (dd, J = 3.7, 0.9 Hz, 1H), 7.51 (dd, J = 5.0, 0.9 Hz, 1H), 7.15 (dd, J = 4.8, 3.9 Hz, 1H), 6.86 (dd, J = 8.5, 7.0 Hz, 2H), 4.50 (s, 1H), 3.50 (d, J = 6.2 Hz, 2H), 1.12 (s, 3H) ppm; ^{13}C NMR (151 MHz, $CDCl_3$) δ 163.94 (dt, J = 253.1, 16.6 Hz), 161.06, 161.00 (ddd, J = 252.1, 15.0, 9.1 Hz), 160.97, 159.74, 142.41, 130.82, 130.29, 128.36, 105.67 (td, J = 21.1, 4.7 Hz), 101.96–100.98 (m), 45.01, 25.79, 18.13 ppm; IR ν 3275, 1540, 1512, 1395, 1190, 1042, 820, 772, 689 cm^{-1}; HRMS (ES^+) calculated for $C_{17}H_{11}ClF_3N_5S$ $[M + H]^+$ 410.0449, found 410.0444.

(S)-6-chloro-2-(thiophen-2-yl)-N-(1,1,1-trifluoropropan-2-yl)pyrimidin-4-amine (31).—Synthesized as **21**, starting from 4,6-dichloro-2-(thiophen-2-yl)pyrimidine (**45**) (0.116 g, 0.502 mmol), (*S*)-1,1,1-trifluoropropan-2-amine (0.227 g, 2.01 mmol) and *N,N*-diisopropylethylamine (0.260 g, 2.01 mmol). Reaction mixture was stirred at 90 °C for 18 h. Purification by silica gel column chromatography (hexanes/EtOAc 98:2) afforded the title compound as a white solid (0.024 g, 0.078 mmol, 15%). ^{1}H NMR (600 MHz, $CDCl_3$) δ 7.96 (d, J = 3.8 Hz, 1H), 7.46 (d, J = 5.1 Hz, 1H), 7.11 (t, J = 4.5 Hz, 1H), 6.28 (s, 1H), 5.06–4.99 (m, 2H), 1.43 (d, J = 7.1 Hz, 3H) ppm; ^{13}C NMR (151 MHz, $CDCl_3$) δ 162.27, 161.11, 160.14, 142.24, 130.52, 129.88, 128.23, 125.54 (q, J = 282.0 Hz), 101.48–100.60 (m), 48.62–47.39 (m), 14.65 ppm; IR (KBr) ν 1586, 1562, 1442, 1379, 1136, 1102, 1019, 714 cm^{-1}; HRMS (ES^+) calculated for $C_{11}H_{10}ClF_3N_3S$ $[M + H]^+$ 308.0231, found 308.0229.

4-chloro-2-(thiophen-2-yl)-5-(2,4,6-trifluorophenyl)pyrimidine (32).—To a solution of 4,6-dichloro-2-(thiophen-2-yl)-5-(2,4,6-trifluorophenyl)pyrimidine (**44**) (0.050 g, 0.138 mmol, 1 equiv) in degassed methanol (0.9 mL) was added sodium acetate (0.023 g, 0.277 mmol, 2 equiv) and Palladium on carbon 10% (0.015 g, 0.0138 mmol, 0.1 equiv). Hydrogen was bubbled into the mixture and then reaction was stirred under hydrogen atmosphere for 20 h. The reaction mixture was filtered, concentrated, and the crude material was purified by silica gel column chromatography (hexanes/EtOAc 97:3) to obtain the title compound as a white solid (0.022 g, 0.067 mmol, 49%). ^{1}H NMR (600 MHz, $CDCl_3$) δ 8.54 (s, 1H), 8.10 (dd, J = 3.7, 1.4 Hz, 1H), 7.56 (dd, J = 5.0, 1.4 Hz, 1H), 7.17 (dd, J = 5.1, 3.7 Hz, 1H), 6.86–6.80 (m, 2H) ppm; ^{13}C NMR (151 MHz, $CDCl_3$) δ 163.60 (dt, J = 253.3, 15.3 Hz), 161.93, 161.11, 160.59 (ddd, J = 252.0, 15.0, 8.8 Hz), 159.63, 141.29, 131.76, 131.03, 128.73, 119.49, 108.69–106.20 (m), 100.98 (td, J = 25.3, 5.5 Hz) ppm; IR (KBr) ν 1594, 1573, 1535, 1439, 1403, 1121, 1034 cm^{-1}; HRMS (ES^+) calculated for $C_{14}H_7ClF_3N_2S$ $[M + H]^+$ 326.9965, found 326.9963. *Diethyl 2-(2,4,6-trifluorophenyl)malonate (**33**).* To a suspension of NaH (60 % in mineral oil, 1 equiv) in anhydrous 1,4-dioxane (previously degassed with N_2) (1.75 mol/L from aryl bromide derivate) at 60 °C under N_2 was slowly added diethyl malonate (9.13 g, 57 mmol, 3 equiv) and 2-bromo-1,3,5-trifluorobenzene (4.00 g, 19 mmol, 1 equiv). Purification by silica gel column chromatography (hexanes/EtOAc 70:30) afforded the title compound as a colourless oil (3.668 g, 12.64 mmol, 66%). ^{1}H NMR (500 MHz, $CDCl_3$) δ 6.71 (t, J = 8.8 Hz, 2H), 4.90 (s, 1H), 4.26 (q, J = 7.1 Hz, 4H), 1.28 (t, J = 7.2 Hz, 6H) ppm.

2-(4,6-dichloro-5-(2,4,6-trifluorophenyl)pyrimidin-2-yl)quinoline (40).—A mixture of diethyl 2-(2,4,6-trifluorophenyl)malonate (**33**) (0.250 g, 0.86 mmol, 1 equiv), quinoline-2-

carboximidamide hydrochloride (**35**) (0.187 g, 0.903 mmol, 1.05 equiv) and tributylamine (0.172 g, 0.929 mmol, 1.08 equiv) was stirred in a sealed tube at 180 °C for 1 h. After cooling at 110 °C, phosphorus oxychloride (0.396 g, 2.58 mmol, 3 equiv) was added dropwise and the mixture was stirred at 100 °C for 16 h. Then, the reaction was cooled to RT and slowly diluted with a mixture of water and toluene (8.6 ml, 6:5). The aqueous phase was extracted with EtOAc (×3), and the combined organic layers were washed with brine (×2), dried over MgSO4, filtered, and concentrated. Purification by silica gel column chromatography (hexanes/EtOAc 100:0 to 80:20) afforded the title compound as a white solid (0.135 g, 0.332 mmol, 35%). ^{1}H NMR (500 MHz; $CDCl_3$) δ 8.55 (d, J = 8.6 Hz, 1H), 8.35 (d, J = 8.5 Hz, 1H), 8.31 (d, J = 8.6 Hz, 1H), 7.84 (d, J = 8.1 Hz, 1H), 7.75 (td, J = 7.7, 1.3 Hz, 1H), 7.59 (t, J = 7.5 Hz, 1H), 6.84 (dd, J = 8.5, 7.3 Hz, 2H) ppm; ^{13}C NMR (126 MHz; $CDCl_3$) δ 164.15 (dt, J = 253.4, 15.0 Hz), 164.14, 163.49, 160.22 (ddd, J = 252.4, 15.2, 9.0 Hz), 151.78, 148.25, 137.42, 131.02, 130.16, 129.02, 128.42, 127.54, 121.56, 120.98, 107.01 (td, J = 20.5, 4.7 Hz), 101.28–100.84 (m) ppm; MS (ES^+) calculated for $C_{19}H_9Cl_2F_3N_3$ $[M + H]^+$ 406.01, found 406.17.

4,6-dichloro-2-(pyrazin-2-yl)-5-(2,4,6-trifluorophenyl)pyrimidine[33] (41).—A mixture of diethyl 2-(2,4,6-trifluorophenyl)malonate (**33**) (0.679 g, 2.34 mmol) and pyrazine-2-carboximidamide hydrochloride (**36**) (0.390 g, 2.46 mmol) and tributylamine (0.468 g, 2.53 mmol, 1.08 equiv) was stirred in a sealed tube at 180 °C for 1 h. After cooling at 110 °C, phosphorus oxychloride (1.08 g, 7.02 mmol, 3 equiv) was added dropwise and the mixture was stirred at 100 °C for 16 h. Then, the reaction was cooled to RT and slowly diluted with a cold mixture of water and dichloromethane (10 ml, 1:1). The aqueous phase was extracted with EtOAc (×3), and the combined organic layers were washed with brine (×2), dried over $MgSO_4$, filtered, and concentrated. Purification by silica gel column chromatography (hexanes/EtOAc 100:0 to 70:30) afforded the title compound as a brown solid (0.252 g, 0.706 mmol, 30%). ^{1}H NMR (600 MHz, $CDCl_3$) δ 9.74 (d, J = 1.3 Hz, 1H), 8.84 (dd, J = 2.5, 1.5 Hz, 1H), 8.77 (d, J = 2.4 Hz, 1H), 6.91–6.83 (m, 2H) ppm; ^{13}C NMR (151 MHz, $CDCl_3$) δ 164.31 (dt, J = 254.0, 15.1 Hz), 163.71, 162.40, 160.24 (ddd, J = 252.7, 15.2, 8.9 Hz), 147.44, 146.98, 146.05, 144.95, 122.30, 106.76 (td, J = 20.6, 4.9 Hz), 101.47–100.97 (m) ppm.

2-(4,6-dichloro-5-(2,4,6-trifluorophenyl)pyrimidin-2-yl)thiazole (42).—A mixture of diethyl 2-(2,4,6-trifluorophenyl)malonate (**33**) (0.600 g, 2.07 mmol, 1 equiv), isothiazole-5-carboximidamide hydrochloride (**37**) (0.355 g, 2.17 mmol, 4 equiv), and tributylamine (0.172 g, 0.929 mmol, 1.08 equiv) was stirred in a sealed tube at 180 °C for 1 h. After cooling at 110 °C, phosphorus oxychloride (0.952 g, 6.21 mmol, 3 equiv) was added dropwise and the mixture was stirred at 100 °C for 16 h. Then, the reaction was cooled to RT and slowly diluted with a mixture of CH_2Cl_2 and water (1:1). The aqueous phase was extracted with CH_2Cl_2 (×1), the combined organic layers were washed with brine (×3), dried over $MgSO_4$, filtered and concentrated. Purification by silica gel column chromatography (hexanes/EtOAc 90:10) afforded the title compound as a brown solid (0.196 g, 0.541 mmol, 26%). ^{1}H NMR (600 MHz, $CDCl_3$) δ 8.12 (d, J = 3.1 Hz, 1H), 7.67 (d, J = 3.1 Hz, 1H), 6.90–6.82 (m, 2H) ppm; ^{13}C NMR (151 MHz, $CDCl_3$) δ 163.40, 163.11 (dt, J = 610.2,

15.6 Hz), 159.57–159.36 (m), 159.35, 146.09, 125.24, 121.66, 106.82 (td, J = 20.1, 4.5 Hz), 101.78–99.98 (m) ppm.

4,6-dichloro-2-(furan-2-yl)-5-(2,4,6-trifluorophenyl)pyrimidine[33] (43).— Synthesized as **40**, starting from diethyl 2-(2,4,6-trifluorophenyl)malonate (**33**) (0.250 g, 0.86 mmol) and furan-2-carboximidamide hydrochloride (**38**) (0.132 g, 0.903 mmol). Purification by silica gel column chromatography (hexanes/EtOAc 100:0 to 90:10) afforded the title compound as a white solid (0.076 g, 0.220 mmol, 26%). ^{1}H NMR (500 MHz; $CDCl_3$) δ 7.68 (s, 1H), 7.48 (d, J = 3.5 Hz, 1H), 6.85–6.79 (m, 2H), 6.60 (dd, J = 3.5, 1.7 Hz, 1H) ppm; ^{13}C NMR (126 MHz; $CDCl_3$) δ 164.07 (dt, J = 253.2, 15.2 Hz), 162.74, 160.37 (ddd, J = 252.1, 15.0, 8.9 Hz), 157.27, 149.69, 147.08, 118.70, 117.42, 113.00, 107.18 (td, J = 20.9, 4.7 Hz), 100.99 (td, J = 26.3, 3.3 Hz) ppm; MS (ES^+) calculated for $C_{14}H_6Cl_2F_3N_2O$ $[M + H]^+$ 344.98, found 345.09.

4,6-Dichloro-2-(thiophen-2-yl)-5-(2,4,6-trifluorophenyl)pyrimidine (44).— Synthesized as **40**, starting from diethyl 2-(2,4,6-trifluorophenyl)malonate (**33**) (0.250 g, 0.86 mmol) and thiophene-2-carboximidamide hydrochloride (**39**) (147 mg, 0.903 mmol). Purification by silica gel column chromatography (hexanes/EtOAc 100:0 to 90:10) afforded the title compound as a white solid (0.097 g, 0.269 mmol, 31%). ^{1}H NMR (500 MHz; $CDCl_3$) δ 8.13 (dd, J = 3.7, 1.0 Hz, 1H), 7.61 (dd, J = 5.0, 1.0 Hz, 1H), 7.18 (dd, J = 4.8, 3.9 Hz, 1H), 6.87–6.81 (m, 2H) ppm; ^{13}C NMR (126 MHz; $CDCl_3$) δ 162.50, 161.66, 140.15, 132.90, 132.17, 128.87, 118.46, 101.04 (td, J = 26.3, 3.3 Hz) ppm; MS (ES^+) calculated for $C_{14}H_6Cl_2F_3N_2S$ $[M + H]^+$ 360.96, found 361.02.

4,6-dichloro-2-(thiophen-2-yl)pyrimidine (45).—Synthesized as **42**, starting from diethyl malonate (0.281 g, 1.76 mmol) and thiophene-2-carboximidamide hydrochloride (**39**) (0.300 g, 1.84 mmol), purification by silica gel column chromatography (hexanes/EtOAc 99:1 to 97:3) afforded the title compound as a white solid (0.114 g, 0.493 mmol, 28%). ^{1}H NMR (600 MHz, $CDCl_3$) δ 8.06 (d, J = 3.7 Hz, 1H), 7.56 (d, J = 5.0 Hz, 1H), 7.17–7.12 (m, 2H) ppm; ^{13}C NMR (151 MHz, $CDCl_3$) δ 162.08, 161.85, 140.42, 132.38, 131.65, 128.68, 118.04 ppm.

Maintenance of the *S. mansoni* life cycle.

The parasite (NMRI isolate) was maintained by passage though *Biomphalaria glabrata* (NMRI isolate) snails and female LVG Golden Syrian hamsters (infected at 4–6 weeks of age) as intermediate and definitive hosts, respectively.[34, 51] The preparation and maintenance of somules (schistosomula; post-infective larvae)[34, 52, 53] and adults[34, 54] have been described. Use of hamsters was in accordance with a protocol approved by the Institutional Animal Care and Use Committee (IACUC) at the University of California, San Diego.

In vitro phenotypic screening of *S. mansoni* somules and adults.

Somule screens were performed as described in 200 μl Basch medium (Basch, 1981) supplemented with 4% heat-inactivated FBS, 100 U/ml penicillin and 100 μg/ml streptomycin in 96-well round-bottomed plates (Corning Inc., cat. # 3799).[34, 35] Adult screens (approximately five males and 2 females /well) were performed in 2 ml of the same

medium in 24-well plates (Corning Inc., cat. # 3526), as described.[34, 35] Compounds were added in a volume of up 1.0 µl DMSO for somule screens and from 0.5 to 2 µl DMSO for adult screens with extensive mixing. Incubations were maintained for up to 48 h at 37 °C and 5% CO_2. Parasite responses to compound were observed at the indicated time-points in Tables 2 and 3 using a Zeiss Axio Vert A1 inverted microscope. Images and movies were recorded using a Zeiss AxioCam MRc digital camera controlled by Zen 2 (blue edition) software.

The parasite's complex phenotypic responses to compound treatment, incorporating one or more changes in shape, density and motility were observed over time and recorded using a nomenclature of simple descriptors (Table 1).[34-37] To allow for the partially quantitative comparisons of compound effects on the parasite, each descriptor was typically given a value of 1 and these were added up to yield a 'severity score' with a score of 4 (Scheme 1).[35, 37, 55] Descriptors recording severe phenotypes, *i.e.*, death, degeneracy, or for adult parasites specifically, damage to the surface tegument, were automatically awarded the highest score of 4. Paralysis (here meaning immobility) was awarded a score of 2. For adult parasites, WormAssay was also employed to quantify the average motility of worms per well.[38, 39]

Maintenance of HeLa and HEK293 cells.

The HeLa and HEK 293T cell lines (American Type Culture Collection, ATCC) were cultured in DMEM (Invitrogen) supplemented with 10% FBS (Gibco, Carlsbad, CA) and penicillin-streptomycin (1%) at 37 °C and 5% CO_2.

In vitro HeLa and HEK 293T cytotoxicity screenings.

The inhibition of cancer cell proliferation was determined using the Promega CellTiter-Glo® reagent (G7572) according to the manufacturer's recommendation. Compounds in 100% DMSO were diluted in 50 µL DMEM medium in 96-well plates (Corning 3903); a further 50 µL of cells in DMEM were added such that the final DMSO concentration was 1%. Eight-point concentration-response assays (depending on the initial EC_{50} value, ranging from 50 µM to 0.39 µM or from 4 µM to 0.8 nM) were set up. HeLa or HEK 293T cells were then diluted to $1x10^5$ cells/mL in DMEM and dispensed into the previously prepared 96-well plates at 50 µL per well. After 48 h at 37 °C and 5% CO_2, cells were lysed by the addition of 100 µL/well of Cell-titer Glo®. Luminescence was measured in a 2104 EnVision® multilabel plate reader (PerkinElmer). The activity of test compounds was normalized to controls from the same plate. CC_{50} values, *i.e.*, the concentration of compound required to inhibit cell growth by 50%, were calculated using GraphPad Prism software, version 8.3.0 for macOS. Unless otherwise indicated with an asterisk, each assay was performed as singletons in three experimental replicates and means ± SD values are shown.

HEK293 MT-stabilization assay.

Test compounds were assessed for MT-stabilizing activity using the established HEK293 cellular assay in which of acetyl-tubulin levels were measured in cell lysates by ELISA 4 h after compound addition, as previously described.[40, 48]

Supplementary Material

Refer to Web version on PubMed Central for supplementary material.

Acknowledgments

Financial support for this work was provided by NIH-NIAID awards, R21AI133394, R21Al141210 and R21Al126296. The *S. mansoni* life cycle at the CDIPD was supported in part by snails and/or hamsters provided by the NIAID Schistosomiasis Resource Center and that were distributed through BEI Resources under the NIH-NIAID Contract HHSN272201700014I.

Abbreviations Used

MT(s)	microtubule(s)
SAR(s)	structure-activity relationship(s)
AcTub	acetylated α-tubulin

References

1. Gryseels B; Polman K; Clerinx J; Kestens L, Human schistosomiasis. Lancet 2006, 368 (9541), 1106–18. DOI: 10.1016/S0140-6736(06)69440-3. [PubMed: 16997665]
2. Colley DG; Bustinduy AL; Secor WE; King CH, Human schistosomiasis. Lancet2014, 383 (9936), 2253–64. DOI: 10.1016/S0140-6736(13)61949-2. [PubMed: 24698483]
3. https://www.who.int/news-room/fact-sheets/detail/schistosomiasis.
4. McManus DP; Dunne DW; Sacko M; Utzinger J; Vennervald BJ; Zhou XN, Schistosomiasis. Nat Rev Dis Primers 2018, 4 (1), 13. DOI: 10.1038/s41572-018-0013-8. [PubMed: 30093684]
5. Steinmann P; Keiser J; Bos R; Tanner M; Utzinger J, Schistosomiasis and water resources development: systematic review, meta-analysis, and estimates of people at risk. Lancet Infect Dis 2006, 6 (7), 411–25. DOI: 10.1016/S1473-3099(06)70521-7. [PubMed: 16790382]
6. Grimes JE; Croll D; Harrison WE; Utzinger J; Freeman MC; Templeton MR, The relationship between water, sanitation and schistosomiasis: a systematic review and meta-analysis. PLoS neglected tropical diseases 2014, 8 (12), e3296. DOI: 10.1371/journal.pntd.0003296. [PubMed: 25474705]
7. Caffrey CR, Schistosomiasis and its treatment. Future medicinal chemistry 2015, 7 (6), 675–6. DOI: 10.4155/fmc.15.27. [PubMed: 25996057]
8. Barsoum RS; Esmat G; El-Baz T, Human schistosomiasis: clinical perspective: review. J Adv Res 2013, 4 (5), 433–44. DOI: 10.1016/j.jare.2013.01.005. [PubMed: 25685450]
9. Caffrey CR; El-Sakkary N; Mäder P; Krieg R; Becker K; Schlitzer M; Drewry DH; Vennerstrom JL; Grevelding CG, Drug Discovery and Development for Schistosomiasis. In Neglected Tropical Diseases: Drug Discovery and Development, Swinney David; Pollastri Michael; Mannhold Raimund; Buschmann Helmut; Holenz J, Eds. 2019; pp 187–225. DOI: 10.1002/9783527808656.ch8.
10. Meyer T; Sekljic H; Fuchs S; Bothe H; Schollmeyer D; Miculka C, Taste, a new incentive to switch to (R)-praziquantel in schistosomiasis treatment. PLoS neglected tropical diseases 2009, 3 (1), e357. DOI: 10.1371/journal.pntd.0000357. [PubMed: 19159015]
11. Andrews P; Thomas H; Pohlke R; Seubert J, Praziquantel. Med Res Rev 1983, 3 (2), 147–200. [PubMed: 6408323]
12. Gray DJ; McManus DP; Li Y; Williams GM; Bergquist R; Ross AG, Schistosomiasis elimination: lessons from the past guide the future. Lancet Infect Dis 2010, 10 (10), 733–6. DOI: 10.1016/S1473-3099(10)70099-2. [PubMed: 20705513]

13. Sabah AA; Fletcher C; Webbe G; Doenhoff MJ, Schistosoma mansoni: chemotherapy of infections of different ages. Exp Parasitol 1986, 61 (3), 294–303. DOI: 10.1016/0014-4894(86)90184-0. [PubMed: 3086114]

14. Doenhoff MJ; Cioli D; Utzinger J, Praziquantel: mechanisms of action, resistance and new derivatives for schistosomiasis. Current opinion in infectious diseases 2008, 21 (6), 659–67. DOI: 10.1097/QCO.0b013e328318978f. [PubMed: 18978535]

15. Melman SD; Steinauer ML; Cunningham C; Kubatko LS; Mwangi IN; Wynn NB; Mutuku MW; Karanja DM; Colley DG; Black CL; Secor WE; Mkoji GM; Loker ES, Reduced susceptibility to praziquantel among naturally occurring Kenyan isolates of Schistosoma mansoni. PLoS neglected tropical diseases 2009, 3 (8), e504. DOI: 10.1371/journal.pntd.0000504. [PubMed: 19688043]

16. Fennell B; Naughton J; Barlow J; Brennan G; Fairweather I; Hoey E; McFerran N; Trudgett A; Bell A, Microtubules as antiparasitic drug targets. Expert opinion on drug discovery 2008, 3 (5), 501–518. DOI: doi:10.1517/17460441.3.5.501. [PubMed: 23484923]

17. Wiest PM; Tartakoff AM; Aikawa M; Mahmoud AA, Inhibition of surface membrane maturation in schistosomula of Schistosoma mansoni. Proc Natl Acad Sci U S A 1988, 85 (11), 3825–9. DOI: 10.1073/pnas.85.11.3825. [PubMed: 3375243]

18. Schmidt J, Effects of benzimidazole anthelmintics as microtubule-active drugs on the synthesis and transport of surface glycoconjugates in Hymenolepis microstoma, Echinostoma caproni, and Schistosoma mansoni. Parasitology Research 1998, 84 (5), 362–368. DOI: 10.1007/s004360050411. [PubMed: 9610632]

19. Bogitsh BJ, Schistosoma mansoni: colchicine and vinblastine effects on schistosomule digestive tract development in vitro. Exp Parasitol 1977, 43 (1), 180–8. DOI: 10.1016/0014-4894(77)90021-2. [PubMed: 891702]

20. Dumontet C; Jordan MA, Microtubule-binding agents: a dynamic field of cancer therapeutics. Nat Rev Drug Discov 2010, 9 (10), 790–803. DOI: 10.1038/nrd3253. [PubMed: 20885410]

21. Lu Y; Chen J; Xiao M; Li W; Miller DD, An Overview of Tubulin Inhibitors That Interact with the Colchicine Binding Site. Pharmaceutical research 2012, 29 (11), 2943–2971. DOI: 10.1007/s11095-012-0828-z. [PubMed: 22814904]

22. Gigant B; Wang C; Ravelli RBG; Roussi F; Steinmetz MO; Curmi PA; Sobel A; Knossow M, Structural basis for the regulation of tubulin by vinblastine. Nature 2005, 435 (7041), 519–522. DOI: 10.1038/nature03566. [PubMed: 15917812]

23. Sáez-Calvo G; Sharma A; Balaguer F. d. A.; Barasoain I; Rodríguez-Salarichs J; Olieric N; Muñoz-Hernández H; Berbís MÁ; Wendeborn S; Peñalva MA; Matesanz R; Canales Á; Prota AE; Jímenez-Barbero J; Andreu JM; Lamberth C; Steinmetz MO; Díaz JF, Triazolopyrimidines Are Microtubule-Stabilizing Agents that Bind the Vinca Inhibitor Site of Tubulin. Cell Chemical Biology 2017, 24 (6), 737–750 e6. DOI: 10.1016/j.chembiol.2017.05.016. [PubMed: 28579361]

24. Rao S; He L; Chakravarty S; Ojima I; Orr GA; Horwitz SB, Characterization of the Taxol binding site on the microtubule. Identification of Arg(282) in beta-tubulin as the site of photoincorporation of a 7-benzophenone analogue of Taxol. J Biol Chem 1999, 274 (53), 37990–4. [PubMed: 10608867]

25. Edgar RC, MUSCLE: multiple sequence alignment with high accuracy and high throughput. Nucleic Acids Res 2004, 32 (5), 1792–7. DOI: 10.1093/nar/gkh340. [PubMed: 15034147]

26. Madeira F; Park YM; Lee J; Buso N; Gur T; Madhusoodanan N; Basutkar P; Tivey ARN; Potter SC; Finn RD; Lopez R, The EMBL-EBI search and sequence analysis tools APIs in 2019. Nucleic Acids Res 2019, 47 (W1), W636–W641. DOI: 10.1093/nar/gkz268. [PubMed: 30976793]

27. Minh BQ; Schmidt HA; Chernomor O; Schrempf D; Woodhams MD; von Haeseler A; Lanfear R, IQ-TREE 2: New Models and Efficient Methods for Phylogenetic Inference in the Genomic Era. Mol Biol Evol 2020, 37 (5), 1530–1534. DOI: 10.1093/molbev/msaa015. [PubMed: 32011700]

28. Letunic I; Bork P, Interactive Tree Of Life (iTOL) v4: recent updates and new developments. Nucleic Acids Res 2019, 47 (W1), W256–W259. DOI: 10.1093/nar/gkz239. [PubMed: 30931475]

29. Crowley PJ; Lamberth C; Müller U; Wendeborn S; Nebel K; Williams J; Sageot O-A; Carter N; Mathie T; Kempf H-J; Godwin J; Schneiter P; Dobler MR, Synthesis and fungicidal activity of tubulin polymerisation promoters. Part 1: pyrido[2,3-b]pyrazines. Pest. Manag. Sci. 2010, 66, 178–185. [PubMed: 19795441]

30. Lamberth C; Trah S; Wendeborn S; Dumeunier R; Courbot M; Godwin J; Schneiter P, Synthesis and fungicidal activity of tubulin polymerisation promoters. Part 2: Pyridazines. Bioorg. Med. Chem. 2012, 20 (9), 2803–10. DOI: S0968-0896(12)00225-8[pii]10.1016/j.bmc.2012.03.035. [PubMed: 22494843]

31. Lamberth C; Dumeunier R; Trah S; Wendeborn S; Godwin J; Schneiter P; Corran A, Synthesis and fungicidal activity of tubulin polymerisation promoters. Part 3: imidazoles. Bioorg. Med. Chem 2013, 21 (1), 127–34. DOI: 10.1016/j.bmc.2012.10.052. [PubMed: 23218777]

32. Zhang N; Ayral-Kaloustian S; Nguyen T; Afragola J; Hernandez R; Lucas J; Gibbons J; Beyer C, Synthesis and SAR of [1,2,4]triazolo[1,5-a]pyrimidines, a class of anticancer agents with a unique mechanism of tubulin inhibition. J. Med. Chem 2007, 50 (2), 319–27. DOI: 10.1021/jm060717i. [PubMed: 17228873]

33. Zhang N; Ayral-Kaloustian S; Nguyen T; Hernandez R; Lucas J; Discafani C; Beyer C, Synthesis and SAR of 6-chloro-4-fluoroalkylamino-2-heteroaryl-5-(substituted)phenylpyrimidines as anti-cancer agents. Bioorg. Med. Chem 2009, 17 (1), 111–8. DOI: S0968-0896(08)01081-X[pii]10.1016/j.bmc.2008.11.016. [PubMed: 19041247]

34. Abdulla M-H; Ruelas DS; Wolff B; Snedecor J; Lim K-C; Xu F; Renslo AR; Williams J; McKerrow JH; Caffrey CR, Drug Discovery for Schistosomiasis: Hit and Lead Compounds Identified in a Library of Known Drugs by Medium-Throughput Phenotypic Screening. PLoS Neglected Tropical Diseases 2009, 3 (7), e478. DOI: 10.1371/journal.pntd.0000478. [PubMed: 19597541]

35. Long T; Neitz RJ; Beasley R; Kalyanaraman C; Suzuki BM; Jacobson MP; Dissous C; McKerrow JH; Drewry DH; Zuercher WJ; Singh R; Caffrey CR, Structure-Bioactivity Relationship for Benzimidazole Thiophene Inhibitors of Polo-Like Kinase 1 (PLK1), a Potential Drug Target in Schistosoma mansoni. PLoS Negl Trop Dis 2016, 10 (1), e0004356. DOI: 10.1371/journal.pntd.0004356. [PubMed: 26751972]

36. Long T; Rojo-Arreola L; Shi D; El-Sakkary N; Jarnagin K; Rock F; Meewan M; Rascón AA; Lin L; Cunningham KA; Lemieux GA; Podust L; Abagyan R; Ashrafi K; McKerrow JH; Caffrey CR, Phenotypic, chemical and functional characterization of cyclic nucleotide phosphodiesterase 4 (PDE4) as a potential anthelmintic drug target. PLoS Negl Trop Dis 2017, 11 (7), e0005680. DOI: 10.1371/journal.pntd.0005680. [PubMed: 28704396]

37. Kyere-Davies G; Agyare C; Boakye YD; Suzuki BM; Caffrey CR, Effect of Phenotypic Screening of Extracts and Fractions of. J Parasitol Res 2018, 2018, 9431467. DOI: 10.1155/2018/9431467. [PubMed: 29977614]

38. Marcellino C; Gut J; Lim KC; Singh R; McKerrow J; Sakanari J, WormAssay: A Novel Computer Application for Whole-Plate Motion-based Screening of Macroscopic Parasites. 2012, 6 (1), e1494. DOI: 10.1371/journal.pntd.0001494.

39. Bibo-Verdugo B; Wang SC; Almaliti J; Ta AP; Jiang Z; Wong DA; Lietz CB; Suzuki BM; El-Sakkary N; Hook V; Salvesen GS; Gerwick WH; Caffrey CR; O'Donoghue AJ, The Proteasome as a Drug Target in the Metazoan Pathogen,. ACS Infect Dis 2019, 5 (10), 1802–1812. DOI: 10.1021/acsinfecdis.9b00237. [PubMed: 31355632]

40. Kovalevich J; Cornec AS; Yao Y; James M; Crowe A; Lee VM; Trojanowski JQ; Smith AB; Ballatore C; Brunden KR, Characterization of brain-penetrant pyrimidine-containing molecules with differential microtubule-stabilizing activities developed as potential therapeutic agents for Alzheimer's disease and related tauopathies. J. Pharmacol. Exp. Ther 2016, 357 (2), 432–50. DOI: 10.1124/jpet.115.231175. [PubMed: 26980057]

41. Black MM; Baas PW; Humphries S, Dynamics of alpha-tubulin deacetylation in intact neurons. J. Neurosci 1989, 9 (1), 358–368. [PubMed: 2563279]

42. Fukushima N; Furuta D; Hidaka Y; Moriyama R; Tsujiuchi T, Post-translational modifications of tubulin in the nervous system. J Neurochem 2009, 109 (3), 683–93. DOI: 10.1111/j.1471-4159.2009.06013.x. [PubMed: 19250341]

43. Jordan MA; Wilson L, Microtubules as a target for anticancer drugs. Nat. Rev. Cancer 2004, 4 (4), 253–265. [PubMed: 15057285]

44. Chatterji BP; Jindal B; Srivastava S; Panda D, Microtubules as antifungal and antiparasitic drug targets. Expert opinion on therapeutic patents 2011, 21 (2), 167–186. DOI: doi:10.1517/13543776.2011.545349. [PubMed: 21204724]

45. Werbovetz KA, Tubulin as an antiprotozoal drug target. Mini reviews in medicinal chemistry 2002, 2 (6), 519–529. [PubMed: 12370037]

46. Monti L; Wang SC; Oukoloff K; Smith AB; Brunden KR; Caffrey CR; Ballatore C, Brain-Penetrant Triazolopyrimidine and Phenylpyrimidine Microtubule Stabilizers as Potential Leads to Treat Human African Trypanosomiasis. ChemMedChem 2018, 13 (17), 1751–1754. DOI: 10.1002/cmdc.201800404. [PubMed: 29969537]

47. Altschul S; Gish W; Miller W; Myers E; DJ L, Basic local alignment search tool. J Mol Biol . 1990; Vol. 215(3), pp 403–410. DOI: 10.1016/S0022-2836(05)80360-2. [PubMed: 2231712]

48. Lou K; Yao Y; Hoye AT; James MJ; Cornec AS; Hyde E; Gay B; Lee VM; Trojanowski JQ; Smith AB; Brunden KR; Ballatore C, Brain-penetrant, orally bioavailable microtubule-stabilizing small molecules are potential candidate therapeutics for Alzheimer's disease and related tauopathies. J Med Chem 2014, 57 (14), 6116–27. DOI: 10.1021/jm5005623. [PubMed: 24992153]

49. Cornec AS; Monti L; Kovalevich J; Makani V; James MJ; Vijayendran KG; Oukoloff K; Yao Y; Lee VM; Trojanowski JQ; Smith AB; Brunden KR; Ballatore C, Multitargeted Imidazoles: Potential Therapeutic Leads for Alzheimer's and Other Neurodegenerative Diseases. J Med Chem 2017, 60 (12), 5120–5145. DOI: 10.1021/acs.jmedchem.7b00475. [PubMed: 28530811]

50. Oukoloff K; Kovalevich J; Cornec AS; Yao Y; Owyang ZA; James M; Trojanowski JQ; Lee VM; Smith AB; Brunden KR; Ballatore C, Design, synthesis and evaluation of photoactivatable derivatives of microtubule (MT)-active [1,2,4]triazolo[1,5-a]pyrimidines. Bioorg Med Chem Lett 2018, 28 (12), 2180–2183. DOI: 10.1016/j.bmcl.2018.05.010. [PubMed: 29764743]

51. Abdulla MH; Lim KC; Sajid M; McKerrow JH; Caffrey CR, Schistosomiasis mansoni: novel chemotherapy using a cysteine protease inhibitor. PLoS Med 2007, 4 (1), e14. DOI: 10.1371/journal.pmed.0040014. [PubMed: 17214506]

52. Colley DG; Wikel SK, Schistosoma mansoni: simplified method for the production of schistosomules. Exp Parasitol 1974, 35 (1), 44–51. DOI: 10.1016/0014-4894(74)90005-8. [PubMed: 4815018]

53. Stefanić S; Dvořák J; Horn M; Braschi S; Sojka D; Ruelas DS; Suzuki B; Lim KC; Hopkins SD; McKerrow JH; Caffrey CR, RNA interference in Schistosoma mansoni schistosomula: selectivity, sensitivity and operation for larger-scale screening. PLoS Negl Trop Dis 2010, 4 (10), e850. DOI: 10.1371/journal.pntd.0000850. [PubMed: 20976050]

54. Duvall RH; DeWitt WB, An improved perfusion technique for recovering adult schistosomes from laboratory animals. Am J Trop Med Hyg 1967, 16 (4), 483–6. DOI: 10.4269/ajtmh.1967.16.483. [PubMed: 4952149]

55. Fonseca NC; da Cruz LF; da Silva Villela F; do Nascimento Pereira GA; de Siqueira-Neto JL; Kellar D; Suzuki BM; Ray D; de Souza TB; Alves RJ; Sales Júnior PA; Romanha AJ; Murta SM; McKerrow JH; Caffrey CR; de Oliveira RB; Ferreira RS, Synthesis of a sugar-based thiosemicarbazone series and structure-activity relationship versus the parasite cysteine proteases rhodesain, cruzain, and Schistosoma mansoni cathepsin B1. Antimicrob Agents Chemother 2015, 59 (5), 2666–77. DOI: 10.1128/AAC.04601-14. [PubMed: 25712353]

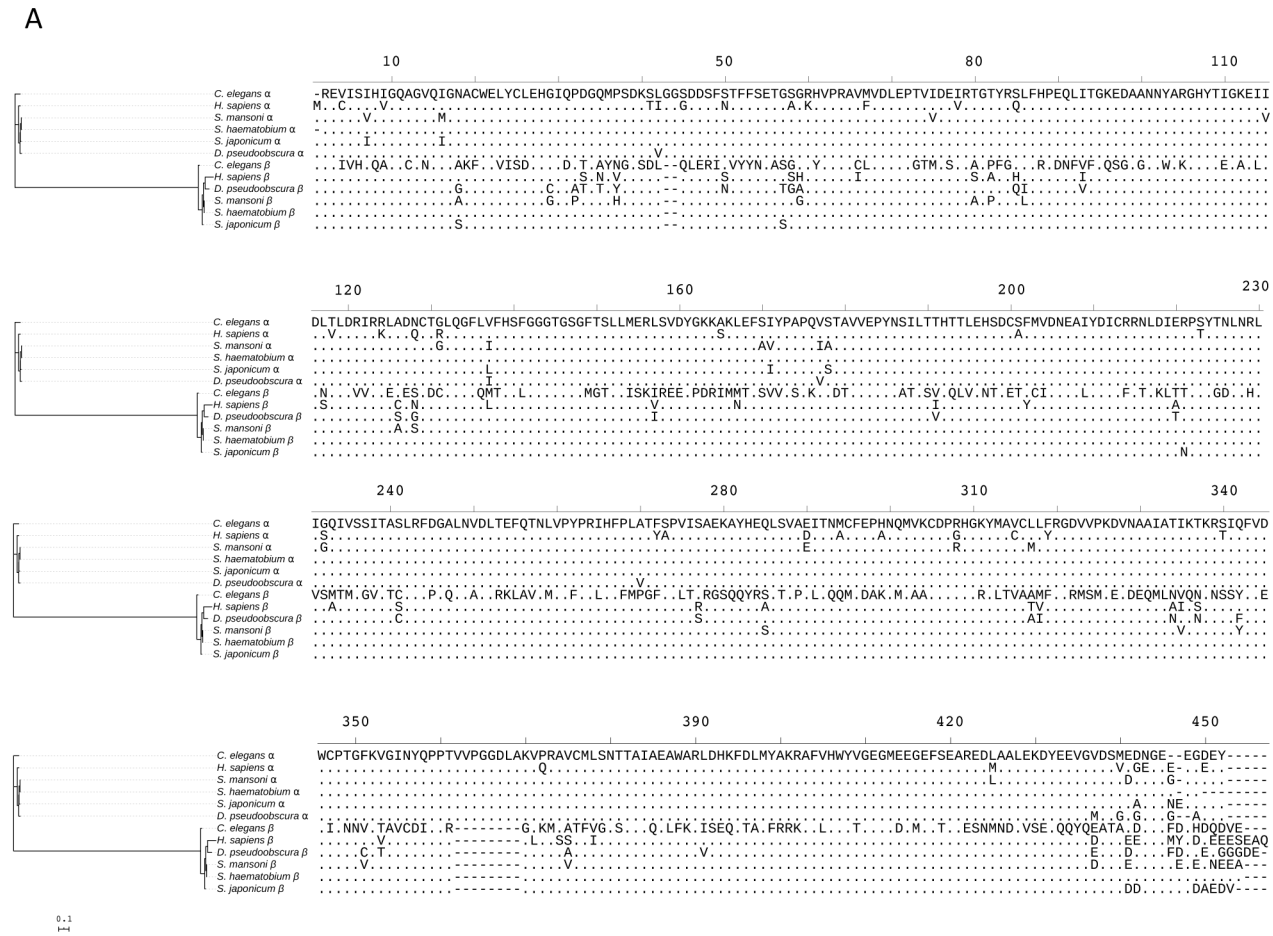

Figure 1. Phylogenetic comparison of α- and β-tubulins from key eukaryotic species.

(A) Full-length alignment of α- and β-tubulin amino acid sequences from *S. mansoni, S. haematobium, S. japonicum, Drosophila pseudoobscura, Caenorhabditis elegans* and *Homo sapiens*. (B) α- and β-tubulin amino acid residues in the proximity of the vinblastine binding site, which is at the interface between the β1 and α2-tubulin subunits. Amino acid residues in contact with a triazolopyrimidine (compound **1** in Ref. 23) in the 5NJH crystal structure[23] are highlighted in blue. The alignment of full-length tubulin sequences was built using MUSCLE[25, 26] and served as the input for the construction of a maximum likelihood phylogenetic tree using IQ-TREE2.[27] The interactive tree of life program (iTOL)[28] was

used to visualise the phylogenetic tree and sequence alignment. The scale bar represents an approximate value for the amino acid substitution rate.

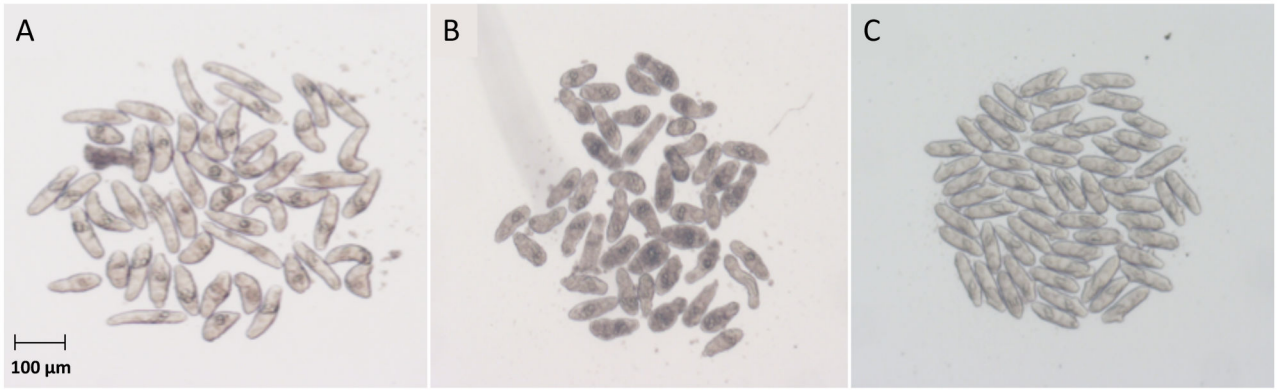

Figure 2. *Schistosoma mansoni* somules 24 h after incubation with example phenylpyrimidines at 10 µM.

(A) DMSO control (0.5% final concentration), (B) **15**, which causes degeneracy, and (C) **25**, which causes rounding and immobility such that the parasites pack closely together in the round-bottomed well.

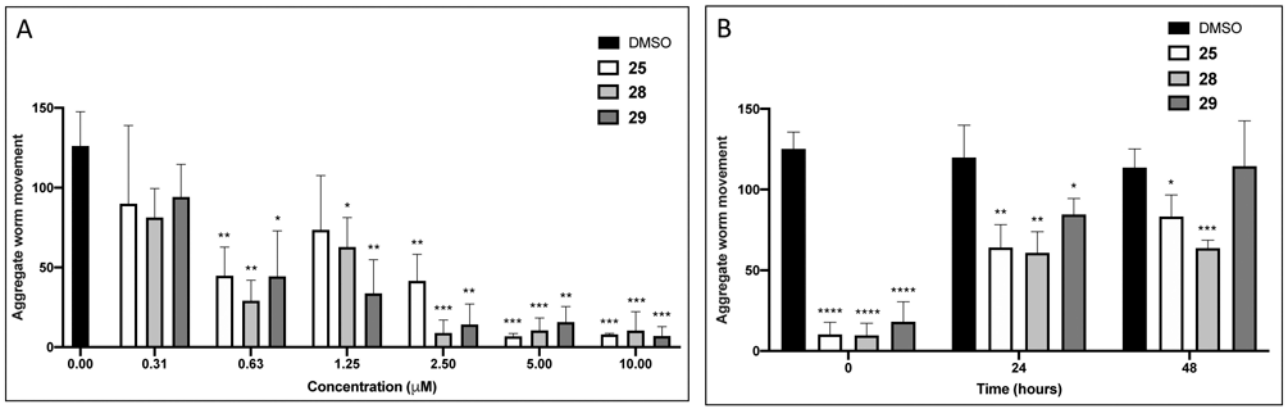

Figure 3.

(A) Concentration-dependent paralysis of adult *S. mansoni* after a 5 h exposure to phenylpyrimidine compounds **25, 28** and **29** at concentrations ranging from 0.31 to 10 μM. Aggregate worm motility was measured using WormAssay's Consensus Voting Luminance Difference algorithm that detects changes in the occupation and vacancy of pixels between a group of video frames.[38] Assays were performed at least three times, each as a singleton, and data are expressed as means ± SD values relative to the 0.5% DMSO control: *p <0.05, **p <0.01 and ***p <0.001 by the unpaired Student's t-test. (B) *S. mansoni* adult worm motility remains suppressed even after removal of **25, 28** or **29**. Parasites were preincubated with 0.5% DMSO or 2 μM of test compound for 5 h. Just prior to exchanging the incubation volume six times (Time 0), worm motility was measured by WormAssay and then again at 24 and 48 h after the exchange. Assays were performed twice, each in duplicate, and data are expressed as means ± SD values relative to the DMSO controls: *p <0.05, **p <0.01, ***p <0.001 and ****p <0.0001 by the unpaired Student's t-test.

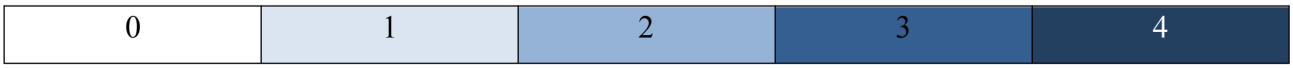

Scheme 1: Severity scores and associated color scheme used in Tables 1 and 2.

The descriptors that contribute to the severity score are presented in Tables 1 and 2 with a glossary of the terms used in the footnote to Table 1.

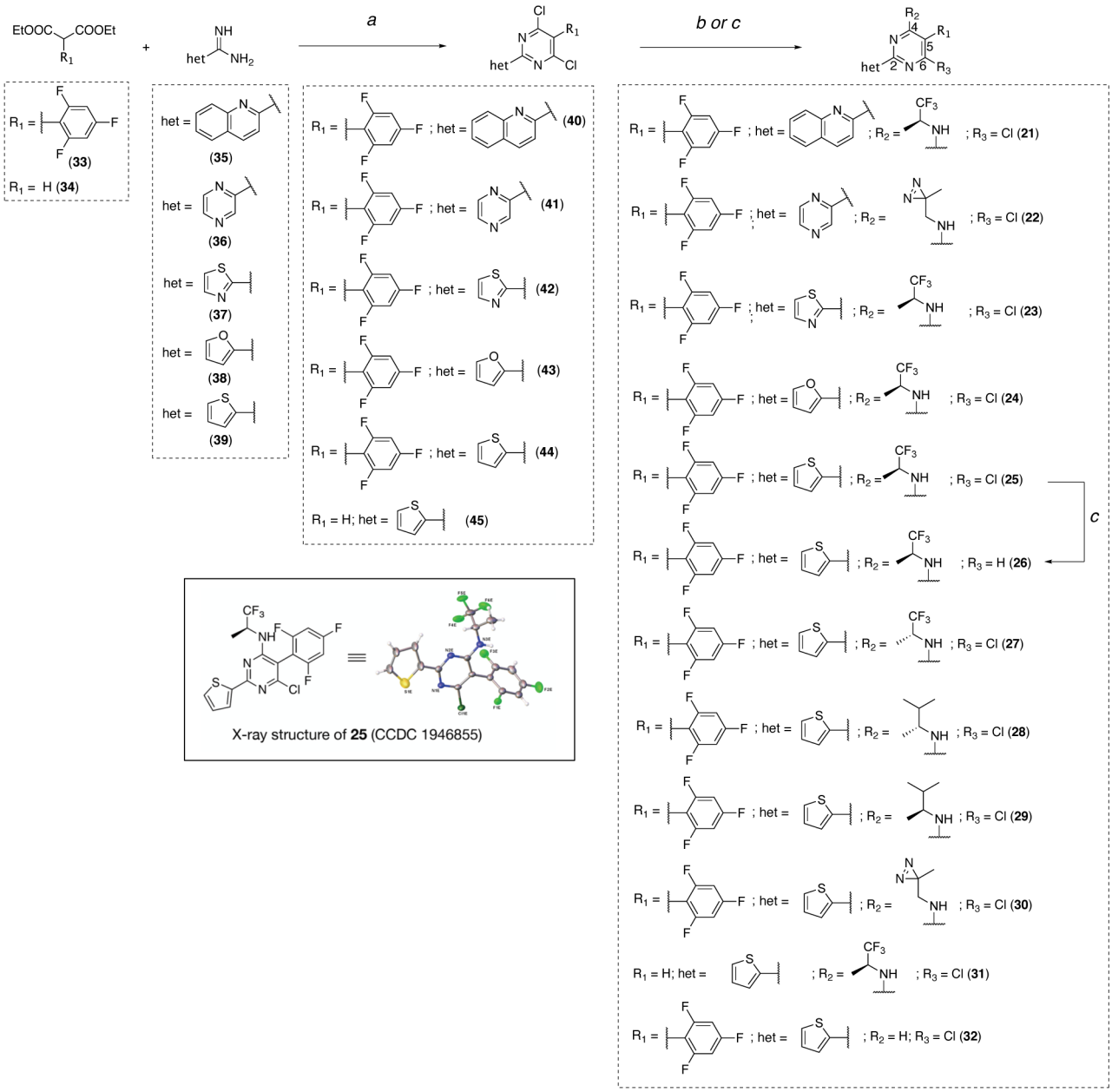

Scheme 2. Reagents and reaction conditions:

(a) (*i*) tributylamine, 180 °C, 1 h; (*ii*) phosphorus oxychloride, 110 °C, 16 h, 26–44% over two steps; (b) appropriate amine, DMF, rt to 90 °C, 1–72 h, 15–100%; (c) **26** or **32**, sodium acetate, Pd/C, H_2, MeOH, 20–48 h, 22–49%.

Table 1.

Phenotypic alterations expressed as descriptors and their associated severity score color for *S. mansoni* somules and adults upon exposure to MT-active agents.

		Somules (1 μM)[a]		Somules (10 μM)[a]		Adults (5 μM)[a]		
Cpd#	**Structure**	**24 h**	**48 h**	**24 h**	**48 h**	**5 h**	**24 h**	**48 h**
1	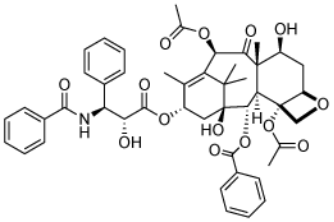	N	N	Dark	R, deg	N	Unc	N
2	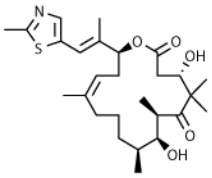	N	N	Unc	R, deg	N	N	N
3	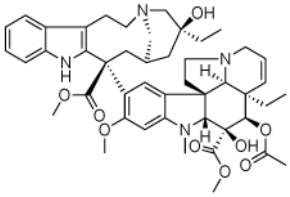	N	N	N	R, dark	N	N	N
4	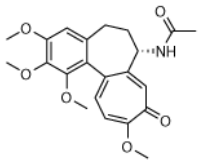	N	N	N	N	S	N	N
5	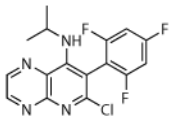	N	N	N	N	N	Unc	Unc
6	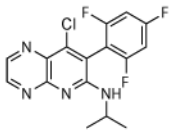	N	N	N	N	N	N	Unc

		Somules (1 μM)[a]		Somules (10 μM)[a]		Adults (5 μM)[a]		
Cpd#	**Structure**	**24 h**	**48 h**	**24 h**	**48 h**	**5 h**	**24 h**	**48 h**
7	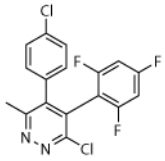	N	Dark	R, deg	R, deg	Unc, on sides	Dark, unc, on sides	Dark, unc, on sides
8	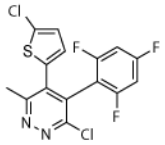	N	Dark	R, deg	R, deg	Unc, on sides	Unc, on sides	Dark, unc, on sides
9	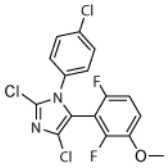	N	N	R, deg	R, deg	Unc, on sides, slight shrunk	Unc, on sides, slight shrunk	Dark, unc, on sides
10	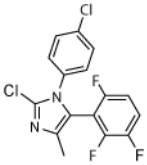	N	N	Unc	R, deg	Unc, on sides	Unc, on sides	Unc, on sides
11	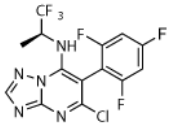	R, unc	N	R, deg	R, deg	N	N	Unc, on sides
12	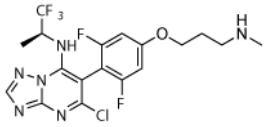	R, deg	R, deg	R, deg	R, deg	N	Dark, unc, slight shrunk	S, on sides, slight shrunk
13	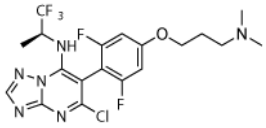	R, dark	R, deg	R, deg,	R, deg	N	Unc	N
14	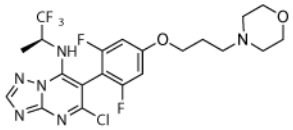	Dark	R, deg	R, deg	R, deg	Unc	Dark, unc	Dark, unc, on sides

		Somules (1 μM)[a]		Somules (10 μM)[a]		Adults (5 μM)[a]		
Cpd#	**Structure**	**24 h**	**48 h**	**24 h**	**48 h**	**5 h**	**24 h**	**48 h**
15	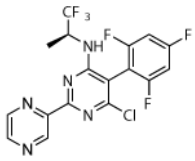	Deg	Deg	Deg	Deg	Dark, unc	Dark, unc	Unc
16	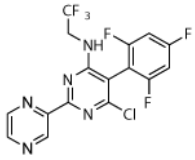	R, deg	R, deg	R, deg,	D	N	S, on sides, slight shrunk	S, on sides
17	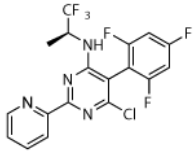	R, deg	R, deg	R, deg	R, deg	N	N	Slight shrunk
18	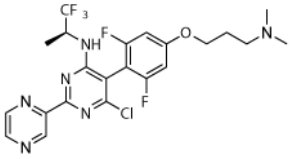	R, deg	R, deg	R, deg	R, deg	S	S, slight shrunk	Slight shrunk
19	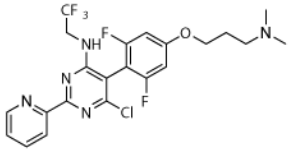	R, deg	R, deg	R, deg	R, deg	N	S, slight shrunk	S, slight shrunk
20	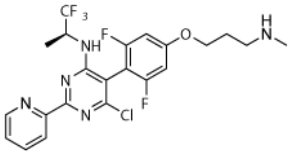	R, deg	R, deg	R, deg	R, deg	Deg, S	Deg, on sides	Deg, on sides
PZQ		Unc	Unc	Deg	Deg	Deg	D	D
DMSO		N	N	N	N	N	N	N

[a]The descriptors and their respective abbreviations are: normal (N); round (R); on sides (adult male worms unable to use oral and/or ventral sucker to adhere to the floor of the well); uncoordinated movements (unc); shrunk (adult worms are not flexing and are smaller than usual); dark; slow (S); immobile (I); degenerate (deg); damage to the surface tegument (teg dam); dead (**D**). Each descriptor is given a value of 1, except for deg and teg dam which are given the maximum value of 4 and I which is given a value of 2. Data are from a minimum of two experiments each in duplicate and representative data are shown.

Table 2.

Activities of phenylpyrimidine congeners against somule and adult *S. mansoni*, their ability to stabilize acetylated tubulin, and mobility measurements by WormAssay.

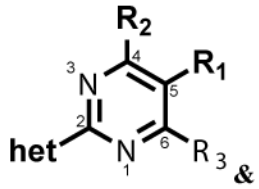

	Structure				Somules (1 μM)[a]		Somules (10 μM)[a]		Adults (5 μM)[a]			Fold-change in acetylated α-tubulin[b]	WormAssay (average adult worm movement ± SD)[c] (5 μM)
Cpd#	**R_1**	**R_2**	**R_3**	**het**	**24 h**	**48 h**	**24 h**	**48 h**	**5 h**	**24 h**	**48 h**	**4 h**	**5 h**
21	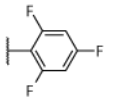		Cl	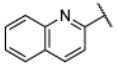	N	N	R, deg	R, deg	N	N	S, on sides	1.95 ± 0.2 (1 μM)	75.3 ± 18.9
22	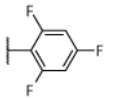		Cl		R, deg	R, deg	R, deg	R, deg	N	N	Unc	2.68 ± 0.04 (1 μM)	131.4 ± 27.4
23	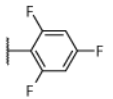		Cl		Deg, unc	Deg, unc	Deg, unc	Deg, unc	Unc, dark[d]	Unc, dark[d]	Unc, dark[d]	4.1 ± 0.3 (1 μM)	62.1 ± 26.4[d]
24	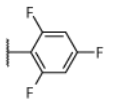		Cl		N	N	N	Deg, unc	S[d]	Unc, on sides[d]	S, dark, on sides[d]	2.7 ± 0.2 (10 μM)	56.0 ± 21.5[d]

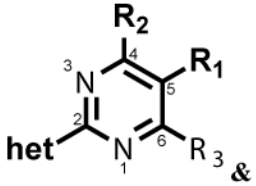

	Structure				Somules (1 μM)[a]		Somules (10 μM)[a]		Adults (5 μM)[a]			Fold-change in acetylated α-tubulin[b]	WormAssay (average adult worm movement ± SD)[c] (5 μM)
Cpd#	R_1	R_2	R_3	het	24 h	48 h	24 h	48 h	5 h	24 h	48 h	4 h	5 h
25	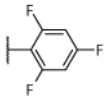		Cl		R, S	R, S	R, I	R, I,	I, on sides	I, on sides	I, on sides	3.0 ± 0.6 (10 μM)	5.5 ± 9.8
26	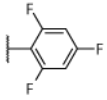		H		R, S	R	R, S	R, S	S[d]	Unc, on sides[d]	S, dark, on sides[d]	NS[e]	11.0 ± 14.7[d]
27	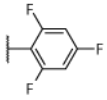		Cl		R, S	R	R, I	R, I	I, on sides	I, on sides	I, on sides	NS	6.3 ± 9.3
28	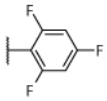		Cl		R, I	R, I	R, I	R, I	I, on sides	I, on sides	I, on sides	NS	2.9 ± 8.8
29	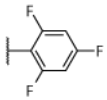		Cl		R, S	R, S	R, I	R, I	I, on sides	I, on sides	I, on sides	NS	5.0 ± 11.5

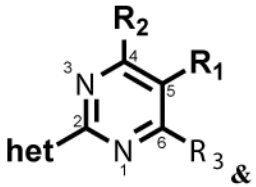

	Structure				Somules (1 μM)[a]		Somules (10 μM)[a]		Adults (5 μM)[a]			Fold-change in acetylated α-tubulin[b]	WormAssay (average adult worm movement ± SD)[c] (5 μM)
Cpd#	**R_1**	**R_2**	**R_3**	**het**	**24 h**	**48 h**	**24 h**	**48 h**	**5 h**	**24 h**	**48 h**	**4 h**	**5 h**
30	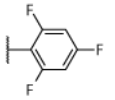	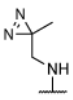	Cl		S	S, R	R, I	R, I	S, on sides	S, on sides	S, on sides	2.25 ± 0.51 (10 μM)	12.9 ± 18.1
31	H		Cl		R, unc	N	R, unc	N	N	N	N	NS	89.0 ± 18.6
32	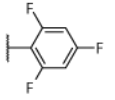	H	Cl		N	N	R, S	N	N	N	N	NS	78.0 ± 20.1
PZQ					Unc	Unc	Deg	Deg	Deg	D	D	NT^f	1.8 ± 5.1
DMSO					N	N	N	N	N	N	N		104.1 ± 24.4

[a] Descriptors are listed in the footnote to Table 1 and their corresponding severity scores are provided in Scheme 1. Data are from a minimum of two experiments each in duplicate and representative data are shown.

[b] ELISA measured the relative changes in acetylated α-tubulin levels after incubation of HEK293 cells with compound for 4 h. Compounds were assessed in triplicate wells within a single experiment.

[c] WormAssay employed a movie camera connected to a Mac computer and an open source software to record the average motion of adult worms in each well.[38, 39]

[d] Assays performed at 10 μM.

[e] NS = Non-significant; changes in AcTub levels observed after 4 h of incubation with either 1 or 10 μM of test compound did not reach statistical significance as determined by one-way ANOVA.

[f] NT = not tested

Table 3.

Cytotoxicity of phenylpyrimidine analogues against HeLa and HEK293 cells.

	HeLa CC_{50} (μM)[a] ± SD values	**HEK293 CC_{50} (μM)[a] ± SD values**
Cpd#	**48 h**	**48 h**
12	0.011 ± 0.379	0.028 ± 0.165
22	0.04 ± 0.012	0.050 ± 0.010
23	0.006 ± 0.001	0.008 ± 0.002
25	1.66 ± 0.612	1.27 ± 0.106
26	> 100	>50*
27	27.7 ± 10.4	29.4*
28	17.4 ± 2.00	26.8*
29	8.78 ± 1.39	29.1*
30	3.89 ± 1.86	1.27 ± 0.035

[a]Half maximal cytotoxicity concentrations (CC_{50}) were determined from eight-point dose-response curves. Assays were conducted as singletons in three experimental replicates and the means ± SD values are reported except for those marked with an asterisk (*) which are the means of two experimental replicates. Compound **12** (cevipabulin[32]) was used as a positive control.